The NCA-1 ion channel functions downstream of G_q and Rho to regulate locomotion in *C. elegans*

Irini Topalidou[*], Pin-An Chen[†], Kirsten Cooper[*,1], Shigeki Watanabe[†,2], Erik M. Jorgensen[†], Michael Ailion[*]

[*]Department of Biochemistry, University of Washington, Seattle, WA 98195

[†]Howard Hughes Medical Institute, Department of Biology, University of Utah, Salt Lake City, UT 84112

[1]Current Address: Fred Hutchinson Cancer Research Center, Seattle, WA 98109

[2]Current Address: Department of Cell Biology, Johns Hopkins University, Baltimore, MD 21205

16 Running Title: Gq signaling activates NCA-1 through Rho

17

18 key words: G_q signaling, Rho small GTPase, NCA/NALCN ion channel, *C. elegans*, G protein

19

20 Corresponding author:

21 Michael Ailion

22 Department of Biochemistry

23 University of Washington

24 Box 357350

25 1705 NE Pacific St

26 Seattle, WA 98195

27 Phone: 206-685-0111

28 email: mailion@uw.edu

29

30 **Abstract**

31 The heterotrimeric G protein G_q positively regulates neuronal activity and synaptic
32 transmission. Previously, the Rho guanine nucleotide exchange factor Trio was identified as a
33 direct effector of G_q that acts in parallel to the canonical G_q effector phospholipase C. Here we
34 examine how Trio and Rho act to stimulate neuronal activity downstream of G_q in the nematode
35 *Caenorhabditis elegans*. Through two forward genetic screens, we identify the cation channel
36 NCA-1/NALCN as a downstream target of the G_q/Rho pathway. By performing genetic epistasis
37 analysis using dominant activating mutations and recessive loss-of-function mutations in the
38 members of this pathway, we show that NCA-1 acts downstream of G_q in a linear pathway.
39 Through cell-specific rescue experiments, we show that function of this channel in head
40 acetylcholine neurons is sufficient for normal locomotion in *C. elegans*. Our results suggest that
41 NCA-1 is a physiologically relevant target of neuronal G_q/Rho signaling in *C. elegans*.

42

43 **Introduction**

44 Heterotrimeric G protein pathways play central roles in altering neuronal activity and
45 synaptic transmission in response to experience or changes in the environment. G_q is one of the
46 four types of heterotrimeric G proteins alpha subunits in animals (Wilkie *et al.* 1992) and is widely
47 expressed in the mammalian brain (Wilkie *et al.* 1991) where it typically acts to stimulate neuronal
48 activity and synaptic transmission (Krause *et al.* 2002; Gamper *et al.* 2004; Coulon *et al.* 2010).
49 These roles are conserved in the nematode *C. elegans*. Unlike mammals which have four
50 members of the G_q family, *C. elegans* has only a single $G_q\alpha$ (Brundage *et al.* 1996). In *C. elegans*,
51 loss-of-function and gain-of-function mutants in the single $G_q\alpha$ gene *egl-30* are viable but have
52 strong neuronal phenotypes, affecting locomotion, egg-laying, and sensory behaviors (Brundage
53 *et al.* 1996; Lackner *et al.* 1999; Bastiani *et al.* 2003; Matsuki *et al.* 2006; Esposito *et al.* 2010;
54 Adachi *et al.* 2010). We aim to identify the signal transduction pathways and downstream targets
55 by which G_q signaling alters neuronal activity.

56 In the canonical G_q pathway, G_q activates phospholipase Cβ (PLC) to cleave the lipid
57 phosphatidylinositol 4,5,-bisphosphate (PIP2) into diacylglycerol (DAG) and inositol trisphosphate
58 (IP3), each of which can act as a second messenger. This pathway operates in both worms and
59 mammals, but in both systems, a number of PLC-independent effects of G_q have been described,
60 indicating the existence of additional G_q signal transduction pathways (Lackner *et al.* 1999; Miller
61 *et al.* 1999; Vogt *et al.* 2003; Bastiani *et al.* 2003; Sánchez-Fernández *et al.* 2014). Using a
62 genetic screen for suppressors of activated G_q, we identified the Rho guanine nucleotide
63 exchange factor (GEF) Trio as a direct effector of G_q in a second major G_q signal transduction
64 pathway independent of the canonical PLC pathway (Williams *et al.* 2007). Biochemical and
65 structural studies demonstrated that G_q directly binds and activates RhoGEF proteins in both
66 worms and mammals, indicating that this new G_q pathway is conserved (Lutz *et al.* 2005; Williams
67 *et al.* 2007; Lutz *et al.* 2007).

68 G_q activation of the Trio RhoGEF leads to activation of the small GTP-binding protein Rho,
69 a major cellular switch that affects a number of cellular processes, ranging from regulation of the
70 cytoskeleton to transcription (Etienne-Manneville and Hall 2002; Jaffe and Hall 2005). In *C.*
71 *elegans* neurons, Rho has been shown to regulate synaptic transmission downstream of the G_{12}-
72 class G protein GPA-12 via at least two pathways, one dependent on the diacylglycerol kinase
73 DGK-1 and one independent of DGK-1 (McMullan *et al.* 2006; Hiley *et al.* 2006). Here we
74 investigate what targets operate downstream of Rho in the G_q signaling pathway to regulate
75 neuronal activity. Through two forward genetic screens, we identify the cation channel NCA-1
76 (NALCN in mammals) as a downstream target of the G_q/Rho pathway. The NCA-1/NALCN
77 channel is a relative of voltage-gated cation channels that has been suggested to be a sodium
78 leak channel required for the propagation of neuronal excitation and the fidelity of synaptic
79 transmission (Lu *et al.* 2007; Jospin *et al.* 2007; Yeh *et al.* 2008). However, there is controversy
80 over the current carried by NALCN and whether it is indeed a sodium leak channel (Senatore *et*
81 *al.* 2013; Senatore and Spafford 2013; Boone *et al.* 2014). It is also unclear how NALCN is gated
82 and what pathways activate the channel. Two studies have shown that NALCN-dependent
83 currents can be activated by G protein-coupled receptors, albeit independently of G proteins (Lu *et*
84 *al.* 2009; Swayne *et al.* 2009), and another study showed that the NALCN leak current can be
85 activated by low extracellular calcium via a G protein-dependent pathway (Lu *et al.* 2010). Our
86 data presented here suggest that NCA-1 can be activated by Rho acting downstream of G_q in a
87 linear pathway.
88

Materials and Methods

Strains

Worm strains were cultured and maintained using standard methods (Brenner, 1974). A complete list of strains and mutations used is provided in the strain list (Table S1).

Isolation of suppressors of activated G_q

We performed an ENU mutagenesis to screen for suppressors of the hyperactive locomotion of an activated G_q mutant, *egl-30(tg26)* (Ailion *et al.* 2014). From approximately 47,000 mutagenized haploid genomes, we isolated 10 mutants that had a fainter phenotype when outcrossed away from the *egl-30(tg26)* mutation. By mapping and complementation testing, we assigned these ten mutants to three genes: three *unc-79* mutants (*yak37*, *yak61*, and *yak73*), six *unc-80* mutants (*ox329*, *ox330*, *yak8*, *yak35*, *yak36*, and *yak56*) and one *nlf-1* mutant (*ox327*).

Isolation of suppressors of activated G_o

We first isolated suppressors of the activated G_o mutant *unc-109(n499)* by building double mutants of *unc-109(n499)* with the activated G_q allele *egl-30(tg26)*. Unlike *unc-109(n499)* homozygotes which are lethal, *egl-30(tg26) unc-109(n499)* homozygotes are viable, but paralyzed and sterile, indicating that activated G_q partially suppresses activated G_o, consistent with the model that these two G proteins act antagonistically. We built a balanced heterozygote strain *egl-30(tg26) unc-109(n499)/egl-30(tg26) unc-13(e51) gld-1(q126)* which has an “unmotivated” phenotype in which the worms move infrequently and slowly. We mutagenized these animals with ENU and screened for F1 progeny that moved better. From a screen of approximately 16,000 mutagenized haploid genomes, we isolated two apparent *unc-109* intragenic mutants, *ox303* and *ox304*. *ox303* is a strong *unc-109* loss-of-function allele, as evidenced by the fact that *egl-30(tg26) unc-109(n499 ox303)/egl-30(tg26) unc-13(e51) gld-1(q126)* mutants resembled *egl-30(tg26)*

115 mutants (i.e. hyperactive). Additionally, *unc-109(n499 ox303)* mutants themselves are hyperactive
116 in an otherwise wild-type background. *ox304*, however, appears to be a partial loss-of-function
117 mutant, because the *egl-30(tg26) unc-109(n499 ox304)/egl-30(tg26) unc-13(e51) gld-1(q126)*
118 mutant moves better than the *egl-30(tg26) unc-109(n499)/egl-30(tg26) unc-13(e51) gld-1(q126)*
119 parent strain, but is not hyperactive like the *egl-30(tg26)* strain. Also, *unc-109(n499 ox304)*
120 homozygote animals on their own are viable but are almost paralyzed and show very little
121 spontaneous movement, with a typical straight posture. However, when stimulated by transfer to a
122 new plate, the *unc-109(n499 ox304)* mutant is surprisingly capable of coordinated movements.
123 This strain was used for mapping and sequencing experiments that demonstrated that *unc-109* is
124 allelic to *goa-1*, encoding the worm G_o ortholog (see below). The *unc-109(n499 ox304)* strain was
125 also used as the starting point for a second screen to isolate extragenic suppressors of activated
126 G_o.

127 Previously, a screen for suppressors of activated *goa-1* was performed using heat-shock
128 induced expression of an activated *goa-1* transgene (Hajdu-Cronin *et al.* 1999). This screen
129 isolated many alleles of *dgk-1*, encoding diacyclglycerol kinase, but only a single allele of *eat-16*,
130 encoding a regulator of G protein signaling (RGS) protein that negatively regulates G_q (Hajdu-
131 Cronin *et al.* 1999), along with mutants in three genes needed for expression of the heat-shock
132 *goa-1* transgene (Hajdu-Cronin *et al.* 2004). Because of the strong bias of this screen for isolating
133 alleles of *dgk-1*, we used the *goa-1(n499 ox304*) strain to perform a screen for suppressors of
134 activated G_o that did not involve overexpression of *goa-1* or rely on expression of a heat-shocked
135 induced *goa-1* transgene. We performed ENU mutagenesis of *goa-1(n499 ox304*) and isolated F2
136 animals that were not paralyzed. From a screen of approximately 24,000 mutagenized haploid
137 genomes, we isolated 17 suppressors, 9 with a relatively stronger suppression phenotype and 8
138 that were weaker. Of the 9 stronger suppressors, we isolated two alleles of *eat-16* (*ox359*, *ox360*),
139 three alleles of the BK type potassium channel *slo-1* (*ox357*, *ox358*, *ox368*), one allele of the
140 innexin *unc-9* (*ox353*), one gain-of-function allele in the ion channel gene *nca-1* (*ox352*), and two

141 mutants that were mapped to chromosomal regions distinct from the other mutations listed above,
142 but not further characterized (*ox356*, *ox364*).
143
144 **Mapping and cloning *unc-109(n499)***
145 *unc-109* was shown to be allelic to *goa-1*. First, we performed SNP mapping of both *unc-*
146 *109(n499)* and its intragenic revertant *unc-109(n499 ox303)*, using the Hawaiian strain CB4856 as
147 described (Davis *et al.* 2005). These experiments mapped *unc-109* to an approximately 1 Mb
148 region in the middle of chromosome I between SNPs on cosmids D2092 and T24B1 (SNPs CE1-
149 15 and T24B1[1]). A good candidate in this region was *goa-1*. We confirmed that *unc-109* was
150 indeed *goa-1* by sequencing the three *unc-109* mutants: the gain-of-function allele *n499* carries a
151 point mutation that leads to an R179C missense mutation, affecting a conserved arginine residue
152 shown to be important for the GTPase activity of G proteins (Coleman *et al.* 1994); the partial loss-
153 of-function allele *ox304* carries a point mutation leading to a W259R missense mutation; and the
154 strong loss-of-function allele *ox303* carries a one basepair deletion that leads to a premature stop
155 32 amino acids from the C-terminal.
156
157 **Mapping and cloning *nlf-1(ox327)***
158 We mapped the *ox327* mutation using single nucleotide polymorphisms (SNPs) in the
159 Hawaiian strain CB4856 as described (Davis et al., 2005). The *ox327* mutation was mapped to an
160 approximately 459 kb region on the left arm of the X chromosome between SNPs on cosmids
161 F39H12 and C52B11 (SNPs F39H12[4] and pkP6101). This region included 74 predicted protein-
162 coding genes. We injected cosmids spanning this region and found that injection of cosmid F55A4
163 rescued the *ox327* mutant phenotype. We performed RNAi to the genes on this cosmid in the *eri-*
164 *1(mg366) lin-15(n744)* strain that has enhanced RNAi and found that RNAi of the gene F55A4.2
165 caused a weak fainter phenotype. We sequenced F55A4.2 in the *ox327* mutant and found a T to
166 A transversion mutation in exon 1, leading to a premature stop codon at amino acid C59. We also

167 rescued the *ox327* mutant with a transgene carrying only F55A4.2, confirming the gene
168 identification. We subsequently obtained a deletion allele *tm3631* that has fainter and G_q
169 suppression phenotypes indistinguishable from *ox327*. F55A4.2 was given the gene name *nlf-1*
170 (Xie *et al.* 2013).

171 We obtained six independent *nlf-1* cDNAs that were predicted to be full-length: yk1105g4,
172 yk1159a2, yk1188d11, yk1279a1, yk1521f8, and yk1709b10. Restriction digests suggested that
173 all six were of the same size. We sequenced yk1159a2 and yk1279a1 and both gave the same
174 *nlf-1* exon-intron structure, which differed from the gene-structure on Wormbase WS253 in several
175 ways: *nlf-1* is 4 bp shorter at the 3' end of exon 5, and has a new 154 bp exon (now exon 6) not
176 predicted on Wormbase. *nlf-1* consists of 8 exons and is predicted to encode a protein of 438
177 amino acids. This is identical to the gene structure reported independently (Xie *et al.* 2013). Both
178 sequenced cDNAs had 5'UTRs of 64 bp, with yk1159a2 (but not yk1279a1) being trans-spliced to
179 the SL1 splice leader, and 3'UTRs of 424 bp (yk1279a1) or 429 bp (yk1159a2). The yk1279a1
180 cDNA was mutation-free and was cloned into a Gateway entry vector for use in rescue
181 experiments. The full-length sequence of the yk1279a1 *nlf-1* cDNA was deposited in GenBank
182 under accession # KX808524.

183

184 **Molecular biology and transgenes**

185 A complete list of constructs is provided in the plasmid list (Table S2). Most of the
186 constructs were made using the three slot multisite Gateway system (Invitrogen). For C3
187 transferase constructs, a promoter, an FRT-mCherry-FRT-GFP cassette (pWD178), and the C3
188 transferase-*unc-54* 3'UTR (cloned into a Gateway entry vector from plasmid QT#99) were
189 combined into the pDEST R4-R3 destination vector. For *nlf-1* tissue-specific rescue constructs, a
190 promoter, the *nlf-1* coding sequence (genomic DNA or cDNA), and a C-terminal GFP tag were
191 cloned along with the *unc-54* 3'UTR into the pDEST R4-R3 destination vector. Promoters used
192 were *nlf-1p* (5.7 kb upstream of the ATG), *rab-3p* (all neurons), *unc-17p* (acetylcholine neurons),

193 *unc-17Hp* (head acetylcholine neurons) (Hammarlund *et al.* 2007), *acr-2p* (acetylcholine motor
194 neurons), *unc-17βp* (acetylcholine motor neurons) (Charlie *et al.* 2006), and *glr-1p* (glutamate-
195 receptor interneurons). Extrachromosomal arrays were made by standard transformation methods
196 (Mello *et al.* 1991). Constructs of interest were injected at 10 ng/μl with marker and carrier DNAs
197 added to make a final total concentration of at least 100 ng/μl. For most constructs, we isolated
198 multiple independent insertions that behaved similarly. C3 transferase extrachromosomal arrays
199 were integrated into the genome using X-ray irradiation (4000 rads). Integrated transgenes were
200 mapped to chromosomes and outcrossed twice before further analysis.
201
202 **Locomotion assays**
203 We performed two different assays to measure locomotion. Body bend assays measured
204 the rate of locomotion. Radial locomotion assays measured the radial distance animals moved
205 from a point in a given unit of time, which provides a combined measurement of different aspects
206 of the locomotion phenotype including the rate of locomotion, waveform, and frequency of
207 reversals. Both types of assays were performed on 10 cm plates seeded with thin lawns of OP50
208 bacteria. These plates were prepared by seeding 1.5 ml of stationary phase OP50 bacteria to
209 evenly cover the entire plate surface, and then growing the bacteria for two days at room
210 temperature. Plates were stored at 4° for up to one month before being used. For body bend
211 assays, first-day adult worms were picked to an assay plate, allowed to rest for 30 seconds, and
212 then body bends were counted for one minute. A body bend was defined as the movement of the
213 worm from maximum to minimum amplitude of the sine wave (Miller *et al.* 1999). To minimize
214 variation, all animals in a body bend experiment were assayed on the same plate. For radial
215 locomotion assays, five to eight first-day adults were picked together to the center of a plate to
216 begin the assay (time 0). Positions of the worms were marked on the lid of the plate every ten
217 minutes for up to forty minutes. Following the assay, the distance of each point to the center was

218 measured. For most strains, radial distances did not increase after the first ten minutes of the
219 assay and all data presented here are for the ten-minute time point. Analysis of the data at later
220 time points leads to the same conclusions. For all locomotion assays, the experimenter was blind
221 to the genotypes of the strains being assayed.

222 For Rho inhibition experiments (Figure 1), expression of C3 transferase (C3T) was induced
223 by FLP-mediated recombination. Expression of FLP was induced by heat shock for 1 hr at 34°C,
224 plates were returned to room temperature, and animals were scored for locomotion 4 hrs after the
225 end of the heat shock period. For heat-shock induction of activated Rho (Figure S5), worms were
226 heat shocked for 1 hr at 34°C, returned to room temperature, and scored for locomotion 2 hrs after
227 the end of the heat-shock period.

228

229 **Fainting assays**

230 Backward fainting times were measured by touching a worm on the head with a worm pick
231 to stimulate movement, and measuring the time to faint with a stopwatch. Forward fainting time
232 was measured following a touch on the tail. Fainting was defined by an abrupt stop of movement
233 along with a characteristic straightening of the head (see Figure 5). Alternatively, we touched
234 worms on the head or tail with a pick and counted the number of body bends until the worm
235 fainted. If a worm moved 10 body bends without fainting, we stopped the assay.

236

237 **Imaging and image analysis**

238 Worms were mounted on 2% agarose pads and anesthetized with sodium azide. Images
239 were obtained using a Zeiss Pascal confocal microscope. For quantitative imaging of NCA-1::GFP
240 and NCA-2::GFP (Figure S2), Z-stack projections of the nerve ring axons on one side of the
241 animal were collected and quantified in ImageJ as described (Jospin *et al.* 2007). Dissecting
242 microscope photographs of first-day adult worms were taken at 50X using a Nikon SMZ18
243 microscope equipped with a DS-L3 camera control system.

244 **Statistics**

245 P values were determined using GraphPad Prism 5.0d (GraphPad Software). Normally
246 distributed data sets with multiple comparisons were analyzed by a one-way ANOVA followed by
247 a Bonferroni or Tukey posthoc test to examine selected comparisons or by Dunnett's test if all
248 comparisons were to the wild type control. Non-normally distributed data sets with multiple
249 comparisons were analyzed by a Kruskal-Wallis nonparametric ANOVA followed by Dunn's test to
250 examine selected comparisons. Pairwise data comparisons were analyzed by a two-tailed
251 unpaired t test for normally distributed data or by a two-tailed Mann-Whitney test for non-normally
252 distributed data.

253

254 **Reagent and data availability**

255 Strains and plasmids are shown in Table S1 and Table S2 and are available from the
256 *Caenorhabditis* Genetics Center (CGC) or upon request. The full-length sequence of the
257 yk1279a1 *nlf-1* cDNA was deposited in GenBank under accession # KX808524. The authors state
258 that all data necessary for confirming the conclusions presented in the article are represented fully
259 within the article and Supplemental Material.

260

261 **Results**

262

263 **Inhibition of Rho suppresses activated G_q**

264 Two pieces of data suggested that G_q may regulate locomotion in *C. elegans* through
265 activation of the small G protein Rho. First, both the hyperactive locomotion and tightly wound
266 body posture of the activated G_q mutant *egl-30(tg26)* are suppressed by loss-of-function mutations
267 in the *unc-73* RhoGEF Trio, an activator of Rho (Williams *et al.* 2007). Second, expression of
268 activated Rho as a transgene causes worms to adopt a posture characterized by a tightly coiled,
269 high-amplitude waveform (McMullan *et al.* 2006), reminiscent of the waveform of activated G_q
270 worms (Bastiani *et al.* 2003; Ailion *et al.* 2014). To determine directly whether G_q signals through
271 Rho, we tested whether Rho inhibition suppresses an activated G_q mutant.

272 In *C. elegans,* there is a single gene encoding Rho (*rho-1*). Loss of *rho-1* causes numerous
273 pleiotropic developmental phenotypes and embryonic lethality (Jantsch-Plunger *et al.* 2000). Thus,
274 to bypass the developmental roles and study Rho function in the adult nervous system, we
275 expressed the Rho inhibitor C3 transferase (C3T) only in adult neurons by using the FLP
276 recombinase/FRT system (Davis *et al.* 2008). In this system, temporal control of C3T is achieved
277 through induction of FLP via heat-shock. FLP in turn promotes recombination between FRT sites
278 to lead to expression of C3 transferase in specific neurons (Figure 1A). We expressed C3T in the
279 following classes of neurons: all neurons (*rab-3p*), acetylcholine neurons *(unc-17p*), head
280 acetylcholine neurons (*unc-17Hp*), and acetylcholine motor neurons (*unc-17βp*). mCherry
281 fluorescence confirmed expression in the expected neurons and GFP expression was used to
282 monitor induction of C3T following FLP-mediated recombination.

283 Inhibition of *rho-1* in adult neurons caused a decreased locomotion rate (Figure 1B). This
284 effect was greatest when Rho was inhibited in all neurons, but Rho inhibition in acetylcholine
285 subclasses of neurons also led to slower locomotion. Thus, Rho acts in multiple classes of
286 neurons to promote locomotion in adult worms. In the absence of heat-shock, all strains showed

287 normal wild-type rates of locomotion and did not express any detectable GFP, indicating that
288 these transgenes do not provide leaky expression of C3T in the absence of heat-shock. This
289 confirms that Rho acts post-developmentally in mature neurons to regulate locomotion behavior
290 (McMullan *et al.* 2006).

291 To determine whether Rho acts downstream of G_q signaling, we crossed the C3 transgenes
292 into the background of the activated G_q mutant *egl-30(tg26)*. Inhibition of *rho-1* in all adult neurons
293 suppressed both the posture and hyperactive locomotion of the activated G_q mutant (Figure
294 1C,D). Inhibition of *rho-1* in acetylcholine neurons suppressed the hyperactivity of activated G_q
295 (Figure 1C), but the worms still had a coiled, high-amplitude waveform (Figure 1D). Thus, *rho-1*
296 exhibits genetic interactions consistent with a role in the G_q signaling pathway.

297

298 **Mutations in NCA channel subunits suppress activated G_q**

299 What acts downstream of Rho in the G_q signal transduction pathway? We screened for
300 suppressors of activated Gq and found mutants in three categories: (1) the canonical G_q pathway
301 (such as the PLC *egl-8*); (2) the RhoGEF *unc-73* (Williams *et al.* 2007), and (3) genes that affect
302 dense-core vesicle function (*e.g. unc-31*, *rab-2*, *rund-1*) (Ailion *et al.* 2014; Topalidou *et al.* 2016).
303 Mutations in *unc-73* strongly suppress the high-amplitude waveform of the activated G_q mutant,
304 but mutations in the canonical G_q pathway or in genes that affect dense-core vesicle function only
305 weakly suppress the high-amplitude waveform of the activated G_q mutant (Figure S1). Thus,
306 strong suppression of the high-amplitude waveform of activated G_q may be a specific
307 characteristic of mutations in the Rho pathway, and we hypothesized that downstream targets of
308 Rho in this pathway would also suppress the high-amplitude waveform.

309 To identify possible downstream targets of Rho in the G_q pathway, we examined other
310 mutants isolated from our screen for suppression of the high-amplitude waveform of activated G_q
311 (Figure S1). When crossed away from the activating G_q mutation, several of these mutants had a
312 “fainter” phenotype. Fainter mutants respond to a touch stimulus by moving away, but abruptly

313 stop, that is “faint”, after only a few body bends. The fainter phenotype has been observed only in
314 mutants that reduce the function of the NCA-1 and NCA-2 ion channels (Humphrey *et al.* 2007;
315 Jospin *et al.* 2007; Yeh *et al.* 2008). We found that all our G_q suppressors that strongly
316 suppressed the high-amplitude waveform and had a fainter phenotype were mutants in either *unc-*
317 *79* or *unc-80*, two genes required for function of the NCA channels (Humphrey *et al.* 2007; Jospin
318 *et al.* 2007; Yeh *et al.* 2008). We also isolated a single mutant in the gene *nlf-1* that only weakly
319 suppressed the high-amplitude waveform of activated G_q (Figure S1), but also gave fainters after
320 outcrossing away from the activated G_q mutation. *unc-79* and *unc-80* mutants have a strong
321 fainter phenotype, equivalent to that of a double mutant in *nca-1* and *nca-2*, two genes that
322 encode pore-forming subunits of the NCA channels in *C. elegans* (Humphrey *et al.* 2007; Jospin
323 *et al.* 2007; Yeh *et al.* 2008). Like *unc-79* or *unc-80*, an *nca-1 nca-2* double mutant suppressed the
324 activated G_q mutant. Additionally, *nca-1* on its own suppressed activated G_q, but *nca-2* did not.
325 This suggests that although *nca-1* and *nca-2* are only redundantly required for normal worm
326 locomotion, G_q activation may be specific to channels containing the NCA-1 pore-forming subunit.
327

328 **Cloning and characterization of *nlf-1(ox327)***

329 In addition to the previously known NCA channel subunits *unc-79* and *unc-80*, we also
330 isolated the *ox327* mutant in a gene that had not been previously characterized at the time of our
331 study. We cloned *ox327* by single nucleotide polymorphism (SNP) mapping, RNAi and transgenic
332 rescue experiments (see Materials and Methods), showing that it carries an early stop mutation in
333 the gene *nlf-1*. The *nlf-1(ox327)* and *nlf-1(tm3631)* deletion mutants failed to complement each
334 other and had indistinguishable fainting and G_q suppression phenotypes. *nlf-1* was independently
335 identified by others and encodes an endoplasmic reticulum-localized protein probably involved in
336 proper assembly of the NCA channel, since *nlf-1* mutants had reduced expression levels of GFP-
337 tagged NCA-1 and NCA-2 (Xie *et al.* 2013). We also found that *nlf-1* is required for normal axonal
338 levels of both GFP-tagged NCA-1 and NCA-2 in the nerve ring (Figure S2). Additionally, an *nlf-1*

339 mutation strongly suppressed both the slow locomotion and coiled posture of an activated *nca-1*
340 mutant (Figure 2), demonstrating that *nlf-1* is important for NCA-1 function.

341 *nlf-1* mutants have a weaker fainter phenotype than mutants of *unc-79* or *unc-80*, or the
342 *nca-1 nca-2* double mutant. The *nlf-1* fainting phenotype differs in two ways from those of the
343 stronger fainting mutants. First, *nlf-1* mutants take a longer time to faint following stimulation
344 (Figure 3). Second, while the strong fainting mutants show a similarly strong fainting phenotype in
345 either the forward or backward direction, *nlf-1* mutants faint reliably in the backward direction but
346 take much longer and have more variable fainting in the forward direction (Figure 3), suggesting
347 that *nlf-1* mutations cause a partial loss of function of the NCA channels. Additionally, *nlf-1*
348 mutants have greater spontaneous locomotion activity than *unc-79*, *unc-80* or *nca-1 nca-2* double
349 mutants. To determine how *nlf-1* interacts with NCA mutants, we built *nlf-1(ox327)* double mutants
350 with *unc-79, unc-80*, *nca-1* and *nca-2*. The *nlf-1* mutation did not enhance the *unc-79* or *unc-80*
351 fainter phenotype, suggesting that these mutants act in the same pathway to control fainting.
352 However, *nca-1* strongly enhanced the *nlf-1* fainter phenotype, while *nca-2* had a weak effect on
353 *nlf-1* fainting that was not statistically significant (Figure 3). Neither *nca-1* nor *nca-2* single mutants
354 have a fainter phenotype on their own, but the fact that an *nca-1 nlf-1* double mutant has a strong
355 fainter phenotype suggests that either *nca-1* contributes more than *nca-2* for normal locomotion or
356 that *nlf-1* specifically perturbs function of *nca-2*. Our data presented below are more consistent
357 with the possibility that *nca-1* contributes more than *nca-2* to wildtype locomotion behavior.

358 We determined the cellular expression pattern of *nlf-1* by fusing its promoter to GFP. *nlf-*
359 *1p::GFP* was expressed in most or all neurons, but was not detected in other tissues (Figure S3).
360 This agrees with the expression pattern reported elsewhere (Xie *et al.* 2013). To determine the
361 neuronal focus of the fainter phenotype, we performed rescue experiments in which we
362 determined whether an *nlf-1* mutant could be rescued by expression of a wild-type *nlf-1* cDNA
363 under the control of neuron-specific promoters. Expression of *nlf-1(+)* in all neurons (using the *rab-*
364 *3* promoter) or acetylcholine neurons (using the *unc-17* promoter) fully rescued the *nlf-1* mutant

365 fainter phenotype (Figure 4A). Expression in acetylcholine motor neurons (using the *acr-2* or *unc-*
366 *17β* promoters) did not rescue the fainter phenotype, but expression driven by a head-specific
367 derivative of the *unc-17* promoter (*unc-17Hp*) fully rescued the fainter phenotype, indicating that
368 the action of *nlf-1* in head acetylcholine neurons is sufficient to prevent fainting (Figure 4A).
369 Previously, it was reported that expression of *nlf-1* in premotor interneurons is sufficient to
370 rescue the *nlf-1* mutant fainter phenotype (Xie *et al.* 2013). However, we found that expression of
371 *nlf-1* in premotor interneurons using the *glr-1* promoter (*glr-1p*) only partially rescued the *nlf-1*
372 mutant fainter phenotype and did not fully restore wild-type locomotion (Figure 4B). Fainting
373 behavior was difficult to score in the *glr-1* promoter-rescued *nlf-1* mutant animals because they
374 had sluggish movement and stopped frequently, though generally not with the suddenness and
375 characteristic posture typical of fainters. Though we could blindly score the rescue of fainting in
376 these animals by eye, we saw only weak rescue of the *nlf-1* mutant by *glr-1* promoter expression
377 in our quantitative fainting assays and the effect was not statistically significant (Figure 4B). When
378 we instead measured fainting as the percentage of animals that fainted within ten body bends, we
379 did see a marginally significant rescue by *glr-1* promoter expression (backward fainting: *nlf-1* =
380 92%, *nlf-1; glr-1p::nlf-1(+)* = 68%, P=0.0738, Fisher's exact test; forward fainting: *nlf-1* = 80%, *nlf-*
381 *1; glr-1p::nlf-1(+)* = 48%, P=0.0378, Fisher's exact test). We may be underestimating the rescue of
382 the fainting phenotype by *glr-1* promoter expression due to the difficulty distinguishing the frequent
383 pausing from true fainting. Nevertheless, rescue of the *nlf-1* mutant is clearly stronger by
384 expression in head acetylcholine neurons using the *unc-17H* promoter (Figure 4A). Though our
385 data seem to contradict the previous study reporting that *nlf-1* acts in premotor interneurons (Xie
386 *et al.* 2013), there are several possible explanations. First, like our data, the data in the previous
387 study in fact showed only partial rescue of fainting behavior by expression in premotor
388 interneurons (Xie *et al.* 2013). Second, the premotor interneuron promoter combination used in
389 the previous study (*nmr-1p* + *sra-11p*) leads to expression in several other head interneurons that
390 may contribute to the phenotype. Third, it is possible that rescue is sensitive to expression level

391 and that different levels of expression were achieved in the two studies, leading to different levels
392 of rescue. We conclude that NLF-1 acts in head acetylcholine neurons, including the premotor
393 interneurons, to promote sustained locomotion in the worm. Consistent with this, the premotor
394 command interneurons have recently been shown to have acetylcholine (Pereira *et al.* 2015).
395

396 **Mutations in NCA channel subunits suppress activated Rho**

397 To determine whether NCA mutants act downstream of Rho, we took advantage of an
398 activated Rho mutant (G14V) expressed specifically in the acetylcholine neurons (McMullan *et al.*
399 2006). Like an activated G_q mutant, this activated Rho mutant has an exaggerated waveform. We
400 built double mutants of the activated Rho mutant with mutations in *unc-79*, *unc-80*, *nlf-1* and
401 mutations in the NCA channel subunit genes *nca-1* and *nca-2*. The *nca-1* and *nca-2* genes are
402 redundant for the fainter phenotype because neither mutant has a fainter phenotype individually,
403 but the double mutant has a fainter phenotype indistinguishable from *unc-79* and *unc-80* mutants
404 (Humphrey *et al.* 2007; Jospin *et al.* 2007; Yeh *et al.* 2008). We found that mutations in *unc-79* or
405 *unc-80* strongly suppressed the high-amplitude waveform of activated Rho, as did an *nca-1 nca-2*
406 double mutant (Figure 5). In all cases, the resulting double (or triple) mutants had a fainter
407 phenotype like the single mutants. By contrast, a mutation in *nlf-1* strongly but incompletely
408 suppressed the high-amplitude waveform of activated Rho, consistent with the *nlf-1* mutation
409 causing a partial but incomplete loss of NCA channel function. Unlike an *nlf-1* single mutant, an
410 *nlf-1* double mutant with activated Rho did not have a fainter phenotype. Additionally, a mutation
411 in *nca-1* also strongly but incompletely suppressed the high-amplitude waveform of activated Rho,
412 but a mutation in *nca-2* did not suppress the high-amplitude waveform (Figure 5). Thus, activated
413 Rho may signal primarily through NCA channels formed from the NCA-1 pore-forming subunit.
414 Because an activated Rho mutant has slow locomotion (Figure 6) and *unc-79*, *unc-80*, and
415 *nca-1 nca-2* double mutants also have slow locomotion, it is difficult to determine whether these
416 NCA channel mutants suppress the locomotion phenotype of activated Rho in addition to its

417 waveform. We performed radial locomotion assays that provide a combined measurement of
418 several aspects of the locomotion phenotype, including the rate of movement, frequency of
419 reversals, and amplitude of the waveform (see Materials and Methods). By these assays,
420 mutations in *unc-80* or *nca-1 nca-2* lead to only small increases in the radial distance traveled by
421 an activated Rho mutant and an *nca-2* mutant had no effect (Figure S4). However, a mutation in
422 *nlf-1* much more strongly increased the radial distance traveled by an activated Rho mutant.
423 Because the *nlf-1* mutant is not as slow on its own, we could also directly assay its effect on the
424 rate of locomotion of an activated Rho mutant by counting the number of body bends per minute.
425 An *nlf-1* mutation strongly increased the rate of locomotion of an activated Rho mutant (Figure 6).
426 In fact, the *nlf-1* double mutant with activated Rho had a faster rate of locomotion than either
427 activated Rho or *nlf-1* on its own, similar to the effect of *nlf-1* on the locomotion of an activated
428 *nca-1* mutant (Figure 2B). Additionally, a mutation in *nca-1* strongly increased the locomotion rate
429 of the activated Rho mutant, but a mutation in *nca-2* had no effect (Figure 6), further supporting
430 the idea that NCA channels consisting of the NCA-1 subunit act downstream of G_q and Rho in this
431 pathway.

432 Rho regulates worm locomotion independently of effects on development, as demonstrated
433 by the fact that heat-shock induction of an activated Rho transgene in adults leads to a high-
434 amplitude waveform similar to that seen in worms that express activated Rho in acetylcholine
435 neurons (McMullan *et al.* 2006). Consistent with the idea that NCA-1 acts downstream of Rho,
436 mutations in the fainter genes *unc-79*, *unc-80*, and *nlf-1* suppress the high-amplitude waveform
437 phenotype of heat-shock induced activated Rho (Figure S5A). Additionally, *nlf-1* also suppresses
438 the locomotion defect of heat-shock induced activated Rho (Figure S5B). Thus, Rho regulates
439 worm locomotion via NCA-1 by acting in a non-developmental pathway that operates in adult
440 neurons.

441

442 **A dominant NCA-1 mutation suppresses activated G_o**

443 In *C. elegans*, the G_q pathway is opposed by signaling through the inhibitory G_o protein
444 GOA-1 (Hajdu-Cronin *et al.* 1999; Miller *et al.* 1999). Thus, loss-of-function mutants in *goa-1* are
445 hyperactive and have a high-amplitude waveform, similar to the gain-of-function G_q mutant *egl-*
446 *30(tg26)*. We found that the uncloned dominant mutant *unc-109(n499)* which is paralyzed and
447 resembles loss-of-function mutants in *egl-30* (Park and Horvitz 1986) carries an activating
448 mutation in *goa-1* (see Materials and Methods). The *goa-1(n499)* mutant is paralyzed as a
449 heterozygote, and is lethal as a homozygote (Park and Horvitz 1986). We performed a screen for
450 suppressors of *goa-1(n499)* and isolated a partial intragenic suppressor, *goa-1(n499 ox304*)
451 (Materials and Methods). The *goa-1(n499 ox304)* mutant has a strong movement defect similar to
452 *goa-1(n499)*, but is viable as a homozygote and thus easier to work with than *goa-1(n499)*.
453 We used the *goa-1(n499 ox304*) strain to perform a screen for suppressors of activated G_o
454 (Materials and Methods). Among the suppressors, we isolated a mutant (*ox352*) that was found to
455 be a dominant gain-of-function mutation in the *nca-1* gene (Fig. 2A, Chen et al., personal
456 communication). Thus, activation of NCA-1 suppresses activated G_o whereas loss of NCA-1
457 suppresses activated G_q, both consistent with the model that G_o inhibits G_q and that NCA-1 is a
458 downstream effector of the G_q pathway.
459

460 **Discussion**

461 In this study, we identify the NCA-1 ion channel as a downstream effector of the
462 heterotrimeric G protein G_q. Our genetic epistasis data indicate that G_q activates the RhoGEF Trio
463 and the small GTPase Rho. Rho then acts via an unknown mechanism to activate the NCA-1 ion
464 channel, which is required for normal neuronal activity and synaptic transmission in *C. elegans*
465 (Jospin *et al.* 2007; Yeh *et al.* 2008; Xie *et al.* 2013; Gao *et al.* 2015). Thus, this work identifies a
466 new genetic pathway from G_q to an ion channel that regulates neuronal excitability and synaptic
467 release: G_q → RhoGEF → Rho → NCA-1 (Figure 7). NCA-1 has not been previously identified as
468 an effector of the G_q pathway, so this pathway may give insight into how NCA-1 is activated or
469 regulated.

470 Mutants that eliminate the NCA channels such as *unc-80* or the *nca-1 nca-2* double mutant
471 completely suppress the locomotion and body posture phenotypes of an activated Rho mutant
472 (Figure 5, Figure S4), suggesting that NCA channels act downstream of Rho in a linear pathway.
473 Additionally, channels composed of the pore-forming subunit NCA-1 may be the main target of
474 G_q/Rho signaling. First, loss-of-function mutations in *nca-1* but not *nca-2* partially suppress
475 activated G_q and activated Rho mutants. Second, activating gain-of-function mutants of *nca-1*
476 have phenotypes reminiscent of activated G_q and activated Rho mutants, but no activated mutants
477 in *nca-2* have been isolated. Third, loss-of-function mutations in *nca-1* but not *nca-2* enhance the
478 weaker fainting phenotype of an *nlf-1* mutant which does not fully eliminate function of the NCA
479 channels. Together, these data suggest that although either NCA-1 or NCA-2 activity is sufficient
480 for wild-type locomotion, NCA-1 is likely to be the target of G protein regulation.

481 It is not clear, however, whether Rho activation of NCA-1 is direct or indirect. G_q directly
482 interacts with and activates the RhoGEF and Rho, as shown by the crystal structure of a complex
483 between $G_q\alpha$, RhoGEF, and Rho (Lutz *et al.* 2007). Rho is known to have many possible effectors
484 and actions in cells (Etienne-Manneville and Hall 2002; Jaffe and Hall 2005). In *C. elegans*
485 neurons, Rho has been previously shown to regulate synaptic transmission via at least two

486 pathways, one involving a direct interaction of Rho with the DAG kinase DGK-1 and one that is
487 DGK-1 independent (McMullan *et al.* 2006). A candidate for the link between Rho and NCA-1 is
488 the type I phosphatidylinositol 4-phosphate 5-kinase (PIP5K) that synthesizes the lipid
489 phosphatidylinositol 4,5,-bisphosphate (PIP2). PIP5K is an intriguing candidate for several
490 reasons. First, activation of G_q in mammalian cells has been shown to stimulate the membrane
491 localization and activity of PIP5K via a mechanism that depends on Rho (Chatah and Abrams
492 2001; Weernink *et al.* 2004). Second, in *C. elegans*, mutations eliminating either the NCA
493 channels (*nca-1 nca-2* double mutant) or their accessory subunits (*unc-79* or *unc-80*) suppress
494 mutants in the PIP2 phosphatase synaptojanin (*unc-26*) and also suppress phenotypes caused by
495 overexpression of the PIP5K gene *ppk-1* (Jospin *et al.* 2007). Loss of a PIP2 phosphatase or
496 overexpression of a PIP5K are both predicted to increase levels of PIP2. Since loss of NCA
497 channels suppresses the effects of too much PIP2, it is possible that excessive PIP2 leads to
498 overactivation of NCA channels and that PIP2 might be part of the normal activation mechanism.
499 There are numerous examples of ion channels that are regulated or gated by phosphoinositide
500 lipids such as PIP2 (Balla 2013).

501 The NCA/NALCN ion channel was discovered originally by bioinformatic sequence
502 analyses (Lee *et al.* 1999; Littleton and Ganetzky 2000). It is conserved among all metazoan
503 animals and is evolutionarily-related to the family of voltage-gated sodium and calcium channels
504 (Liebeskind *et al.* 2012), forming a new branch in this super-family. Although the cellular role of
505 the NCA/NALCN channel and how it is gated are not well understood, NALCN and its orthologs
506 are expressed broadly in the nervous system in a number of organisms (Lee *et al.* 1999; Lear *et*
507 *al.* 2005; Humphrey *et al.* 2007; Lu *et al.* 2007; Jospin *et al.* 2007; Yeh *et al.* 2008; Lu and Feng
508 2011; Lutas *et al.* 2016). Moreover, mutations in this channel or its auxiliary subunits lead to
509 defects in rhythmic behaviors in multiple organisms (Lear *et al.* 2005; Lu *et al.* 2007; Jospin *et al.*
510 2007; Yeh *et al.* 2008; Pierce-Shimomura *et al.* 2008; Lear *et al.* 2013; Xie *et al.* 2013; Funato *et*
511 *al.* 2016). Thus, NCA/NALCN is likely to play an important role in controlling membrane

512 excitability. Additionally, NALCN currents have been reported to be activated by two different G
513 protein-coupled receptors (GPCRs), the muscarinic acetylcholine receptor and the substance P
514 receptor, albeit in a G protein-independent fashion (Lu *et al.* 2009; Swayne *et al.* 2009), and by
515 low extracellular calcium via a G protein-dependent pathway (Lu *et al.* 2010). The latter study
516 further showed that expression of an activated G_q mutant inhibited the NALCN sodium leak
517 current, suggesting that high extracellular calcium tonically inhibits NALCN via a G_q-dependent
518 pathway and that low extracellular calcium activates NALCN by relieving this inhibition (Lu *et al.*
519 2010). By contrast, we find that in *C. elegans*, the physiological role of G_q is to activate NCA-1 and
520 show that NCA-1 is a physiologically relevant target of a G_q signaling pathway that acts through
521 Rho.

522 In the last few years, both recessive and dominant human diseases characterized by a
523 range of neurological symptoms including hypotonia, intellectual disability, and seizures have
524 been shown to be caused by mutations in either *NALCN* or *UNC80* (Köroğlu *et al.* 2013; Al-Sayed
525 *et al.* 2013; Chong *et al.* 2015; Aoyagi *et al.* 2015; Shamseldin *et al.* 2016; Stray-Pedersen *et al.*
526 2016; Gal *et al.* 2016; Fukai *et al.* 2016; Karakaya *et al.* 2016; Perez *et al.* 2016; Bend *et al.* 2016;
527 Wang *et al.* 2016). Notably, dominant disease-causing mutations in the NALCN channel were
528 modeled in worms and resemble either dominant activated or loss-of-function NCA mutants such
529 as the ones we use in this study (Aoyagi *et al.* 2015; Bend *et al.* 2016). Human mutations in other
530 components of the pathway we have described may cause similar clinical phenotypes.

531

532 **Acknowledgments**

533 We thank Shohei Mitani for the *nlf-1(tm3631)* mutant; Steve Nurrish for worm strains and
534 plasmids carrying activated Rho or C3 transferase; Ken Miller for a plasmid with the *unc-17β*
535 promoter; Wayne Davis for FLP/FRT plasmids; Yuji Kohara for cDNA clones; the Sanger Center
536 for cosmids; Brooke Jarvie, Jill Hoyt, and Michelle Giarmarco for the isolation of *unc-79* and *unc-*
537 *80* mutations in the G_q suppressor screen; and Dana Miller for the use of her microscope and

538 camera to take worm photographs. Some strains were provided by the CGC, which is funded by
539 NIH Office of Research Infrastructure Programs (P40 OD010440). M.A. is an Ellison Medical
540 Foundation New Scholar. E.M.J. is an Investigator of the Howard Hughes Medical Institute. This
541 work was supported by NIH grants R00 MH082109 to M.A and R01 NS034307 to E.M.J.
542

543 **Figure Legends**

544

545 **Figure 1** Inhibition of Rho in neurons suppresses an activated G_q mutant. (A) Schematic of the
546 FLP/FRT system we used for temporal and spatial expression of the Rho inhibitor C3 transferase
547 (C3T). The transgene in the ‘‘off’’ configuration expresses the mCherry reporter under the control
548 of the promoter sequence but terminates transcription in the *let-858* 3’UTR upstream of GFP-C3T.
549 Expression of the FLP recombinase is induced by heat shock and leads to recombination between
550 the FRT sites and deletion of the intervening *mCherry::let-858* 3’UTR fragment. This leads to
551 transcription of GFP-C3T in the cells driven by the adjacent promoter. We used the pan-neuronal
552 promoter *rab-3p,* acetylcholine neuron promoter *unc-17p,* and head acetylcholine neuron
553 promoter *unc-17Hp.* (B) Inhibition of Rho in adult neurons causes a locomotion defect. Inhibition of
554 Rho by C3 transferase (C3T) in all adult neurons (*rab-3p, oxIs412* transgene), acetylcholine
555 neurons (*unc-17p, oxIs414* transgene) or head acetylcholine neurons (*unc-17Hp, oxIs434*
556 transgene) reduces the locomotion rate of wild type animals. ***, P<0.001, Dunnett’s test. Error
557 bars = SEM; n = 19-20. (C) Inhibition of Rho in all adult neurons (*rab-3p, oxIs412* transgene) or
558 acetylcholine neurons (*unc-17p*, *oxIs414* transgene) led to a significant reduction in the rate of
559 locomotion of the activated G_q mutant *egl-30(tg26)* (here written Gq*). Inhibition of Rho in head
560 acetylcholine neurons (*unc-17Hp*, *oxIs434* transgene) led to a small decrease in Gq* locomotion
561 that was not statistically significant. ***, P<0.001; ns, not significant, P>0.05, Dunnett’s test. Error
562 bars = SEM; n = 10-20. (D) Inhibition of Rho in all adult neurons (*rab-3p*) suppresses the deep
563 body bends of the activated G_q mutant *egl-30(tg26)* (Gq*). Rho inhibition in acetylcholine (*unc-*
564 *17p*) or head acetylcholine (*unc-17Hp*) neurons did not suppress the waveform of Gq*.

565

566 **Figure 2** The *nlf-1(ox327)* mutation suppresses the coiled posture and locomotion defect of the
567 activated NCA-1 mutant *nca-1(ox352*) (Nca*). (A) Photos of first-day adult worms. (B) Body bend

568 assay. (C) Radial locomotion assay. Statistics in B and C: ***, P<0.001, two-tailed Mann-Whitney
569 test. Error bars = SEM, n = 4-8 (panel B), n= 8-26 (panel C).
570
571 **Figure 3** *nlf-1* mutants are weak fainters. *nlf-1(ox327)* mutant animals have a much weaker fainter
572 phenotype than *unc-80(ox330)* or *nca-2(gk5)*; *nca-1(gk9)* double mutants in the forward direction
573 (A) and a slightly weaker fainter phenotype in the backward direction (B). Additionally, *nlf-1*
574 mutants are enhanced by a mutation in *nca-1*, but not *nca-2*. ***, P<0.001; ns, not significant,
575 P>0.05, Dunn's test. Error bars = SEM; n = 20.
576
577 **Figure 4** *nlf-1* acts in head acetylcholine neurons to control locomotion. The *nlf-1* cDNA was
578 expressed in an *nlf-1(ox327)* mutant background using the following promoters: *rab-3* (all neurons,
579 *oxEx1146* transgene), *unc-17* (acetylcholine neurons, *oxEx1149* transgene), *unc-17H* (a
580 derivative of the *unc-17* promoter that lacks the enhancer for ventral cord expression and thus
581 expresses only in head acetylcholine neurons, *oxEx1155* transgene), *unc-17β* (a derivative of
582 the *unc-17* promoter that expresses only in ventral cord acetylcholine neurons, *oxEx1323*
583 transgene), *acr-2* (ventral cord acetylcholine motor neurons, *oxEx1151* transgene), and *glr-1*
584 (interneurons including premotor command interneurons, *oxEx1152* transgene). (A) Expression
585 driven by the *rab-3*, *unc-17*, and *unc-17H* promoters rescued the fainting phenotype of an *nlf-1*
586 mutant in the backward direction. ***, P<0.001, Dunn's test. Error bars = SEM; n = 15. (B)
587 Expression driven by the *glr-1* promoter partially rescued the fainting phenotype of an *nlf-1* mutant
588 in either the backward or forward direction, though the effect was not statistically significant (ns,
589 P>0.05, two-tailed Mann-Whitney tests. Error bars = SEM; n = 25). However, assays of this strain
590 were complicated by slow movement and frequent pauses that were hard to distinguish from true
591 fainting behavior (see text for details).
592

593 **Figure 5** Mutations in NCA channel subunits suppress the high-amplitude waveform of animals
594 expressing activated Rho. Animals expressing an activated Rho mutant (G14V) in acetylcholine
595 neurons (*nzIs29* transgene, written as Rho*) have a high-amplitude waveform. Mutations that
596 eliminate NCA-1 and NCA-2 channel function (*unc-80(ox330)* or *nca-2(gk5)*; *nca-1(gk9)*) strongly
597 suppress the high-amplitude waveform of activated Rho and convert the activated Rho mutants to
598 fainters. Mutations in *nlf-1(ox327)* and *nca-1(gk9)* strongly but incompletely suppress the high-
599 amplitude waveform of activated Rho and these double mutants do not faint. Mutations in *nca-*
600 *2(gk5)* do not suppress the high-amplitude waveform of activated Rho. Mutants in *unc-80*, *nlf-1*,
601 and the *nca-2 nca-1* double mutant have the typical fainter posture characterized by a
602 straightened anterior part of the body.
603
604 **Figure 6** Mutations in *nlf-1* and *nca-1* suppress the locomotion defect of animals expressing
605 activated Rho. Animals expressing an activated Rho mutant (G14V) in acetylcholine neurons
606 (*nzIs29* transgene, written as Rho*) have a slow locomotion rate. The *nlf-1(ox327)* and *nca-1(gk9)*
607 mutations, but not *nca-2(gk5)*, strongly suppress the slow locomotion rate of activated Rho. ***,
608 $P<0.001$, Bonferroni test. Error bars = SEM; n = 16.
609
610 **Figure 7** Model. G_q activates NCA-1 in a linear pathway via the RhoGEF Trio and small G protein
611 Rho. G_q activation of Trio and Rho is direct (solid arrow). Rho activation of NCA-1 is likely to be
612 indirect (dashed arrow). G_o inhibits G_q via the RGS protein EAT-16 (not shown). Thus, loss-of-
613 function mutations in NCA-1, its associated subunits UNC-79 and UNC-80, or the ER-localized
614 assembly factor NLF-1 suppress an activated G_q mutant, whereas a gain-of-function activating
615 mutation in NCA-1 suppresses an activated G_o mutant.
616
617 **Figure S1** Mutations affecting the NCA-1 channel suppress the high-amplitude waveform of the
618 activated G_q mutant *egl-30(tg26)* (Gq*). The *unc-79(yak37)* and *unc-80(ox330)* mutations strongly

619 suppress the high-amplitude waveform of Gq*. The *nca-1(gk9)* and *nlf-1(ox327)* mutations
620 partially suppress the high-amplitude waveform of Gq*. Mutations in genes required for dense-
621 core vesicle biogenesis such as *rund-1(tm3622)* or the canonical G_q pathway such as *egl-*
622 *8(ox333)* only weakly suppress the high-amplitude waveform of Gq*. The *nca-2(gk5)* mutation
623 does not suppress Gq*.
624
625 **Figure S2** *nlf-1* mutants have reduced *nca-1::gfp* and *nca-2::gfp* fluorescence in the nerve ring.
626 Quantification of the nerve ring fluorescence of C-terminally tagged *nca-1::gfp* (transgene *vaIs46*)
627 and *nca-2::gfp* (transgene *vaIs41*) in wild type and *nlf-1(ox327)* mutants. ***, P<0.001, two-tailed
628 unpaired t tests where each mutant strain is compared to its associated wild-type control. Error
629 bars = SEM; n = 11-12.
630
631 **Figure S3** *nlf-1* is expressed widely in the nervous system. A fusion of the *nlf-1* promoter to GFP
632 (transgene *oxEx1144*) is expressed throughout the nervous system, including head and tail
633 neurons, and motor neurons in the ventral nerve cord. No expression is seen in non-neuronal
634 tissues. An L1 stage larval animal is shown with its head to the left.
635
636 **Figure S4** Mutations in NCA channel subunits suppress the locomotion defect of animals
637 expressing activated Rho. Animals expressing an activated Rho mutant (G14V) in acetylcholine
638 neurons (*nzIs29* transgene, written as Rho*) have reduced locomotion as measured in radial
639 locomotion assays. Mutations that eliminate function of the NCA channels (*unc-80(ox330)* or *nca-*
640 *2(gk5)*;*nca-1(gk9)*) increase the radial distance traveled by activated Rho mutants, but the effect is
641 subtle since *unc-80* and *nca-2; nca-1* mutants have reduced locomotion on their own. The *nlf-*
642 *1(ox327)* mutation that partially but incompletely reduces function of the NCA channels strongly
643 suppresses the locomotion defect of activated Rho. ***, P<0.0001, Bonferroni test. Error bars =
644 SEM; n = 5-18.

645

646 **Figure S5** Mutations in NCA channel subunits suppress the high-amplitude waveform and
647 locomotion of adult animals expressing activated Rho. (A) Animals expressing an activated Rho
648 mutant (G14V) only in adults by heat-shock induced expression (*nzIs1* transgene, *hs::Rho**) have
649 a high-amplitude waveform. The *unc-80(ox330)* and *nlf-1(ox327)* mutations strongly suppress the
650 high-amplitude waveform of activated Rho. *unc-80*, but not *nlf-1*, makes the activated Rho animals
651 faint. (B) Animals expressing an activated Rho mutant (G14V) only in adults by heat-shock
652 induced expression (*nzIs1* transgene, *hs::Rho**) have a reduced locomotion rate. The *nlf-1(ox327)*
653 mutation suppresses the reduced locomotion rate of activated Rho. *, P=0.0157, two-tailed
654 unpaired t test. Error bars = SEM; n = 18-30)

655

656 **Literature Cited**

657 Adachi T., Kunitomo H., Tomioka M., Ohno H., Okochi Y., Mori I., Iino Y., 2010 Reversal of salt preference
658 is directed by the insulin/PI3K and Gq/PKC signaling in Caenorhabditis elegans. Genetics **186**:
659 1309–1319.

660 Ailion M., Hannemann M., Dalton S., Pappas A., Watanabe S., Hegermann J., Liu Q., Han H.-F., Gu M.,
661 Goulding M. Q., Sasidharan N., Schuske K., Hullett P., Eimer S., Jorgensen E. M., 2014 Two Rab2
662 interactors regulate dense-core vesicle maturation. Neuron **82**: 167–180.

663 Al-Sayed M. D., Al-Zaidan H., Albakheet A., Hakami H., Kenana R., Al-Yafee Y., Al-Dosary M., Qari A., Al-
664 Sheddi T., Al-Muheiza M., Al-Qubbaj W., Lakmache Y., Al-Hindi H., Ghaziuddin M., Colak D., Kaya
665 N., 2013 Mutations in NALCN cause an autosomal-recessive syndrome with severe hypotonia,
666 speech impairment, and cognitive delay. Am. J. Hum. Genet. **93**: 721–726.

667 Aoyagi K., Rossignol E., Hamdan F. F., Mulcahy B., Xie L., Nagamatsu S., Rouleau G. A., Zhen M.,
668 Michaud J. L., 2015 A Gain-of-Function Mutation in NALCN in a Child with Intellectual Disability,
669 Ataxia, and Arthrogryposis. Hum. Mutat. **36**: 753–757.

670 Balla T., 2013 Phosphoinositides: tiny lipids with giant impact on cell regulation. Physiol. Rev. **93**: 1019–
671 1137.

672 Bastiani C. A., Gharib S., Simon M. I., Sternberg P. W., 2003 Caenorhabditis elegans Galphaq regulates
673 egg-laying behavior via a PLCbeta-independent and serotonin-dependent signaling pathway and
674 likely functions both in the nervous system and in muscle. Genetics **165**: 1805–1822.

675 Bend E. G., Si Y., Stevenson D. A., Bayrak-Toydemir P., Newcomb T. M., Jorgensen E. M., Swoboda K. J.,
676 2016 NALCN channelopathies: Distinguishing gain-of-function and loss-of-function mutations.
677 Neurology **87**: 1131–1139.

678 Boone A. N., Senatore A., Chemin J., Monteil A., Spafford J. D., 2014 Gd3+ and calcium sensitive, sodium
679 leak currents are features of weak membrane-glass seals in patch clamp recordings. PLoS ONE **9**:
680 e98808.

681 Brundage L., Avery L., Katz A., Kim U. J., Mendel J. E., Sternberg P. W., Simon M. I., 1996 Mutations in a
682 C. elegans Gqalpha gene disrupt movement, egg laying, and viability. Neuron **16**: 999–1009.

683 Charlie N. K., Schade M. A., Thomure A. M., Miller K. G., 2006 Presynaptic UNC-31 (CAPS) is required to
684 activate the G alpha(s) pathway of the Caenorhabditis elegans synaptic signaling network. Genetics
685 **172**: 943–961.

686 Chatah N. E., Abrams C. S., 2001 G-protein-coupled receptor activation induces the membrane
687 translocation and activation of phosphatidylinositol-4-phosphate 5-kinase I alpha by a Rac- and
688 Rho-dependent pathway. J. Biol. Chem. **276**: 34059–34065.

689 Chong J. X., McMillin M. J., Shively K. M., Beck A. E., Marvin C. T., Armenteros J. R., Buckingham K. J.,
690 Nkinsi N. T., Boyle E. A., Berry M. N., Bocian M., Foulds N., Uzielli M. L. G., Haldeman-Englert C.,
691 Hennekam R. C. M., Kaplan P., Kline A. D., Mercer C. L., Nowaczyk M. J. M., Klein Wassink-Ruiter
692 J. S., McPherson E. W., Moreno R. A., Scheuerle A. E., Shashi V., Stevens C. A., Carey J. C.,
693 Monteil A., Lory P., Tabor H. K., Smith J. D., Shendure J., Nickerson D. A., University of
694 Washington Center for Mendelian Genomics, Bamshad M. J., 2015 De novo mutations in NALCN
695 cause a syndrome characterized by congenital contractures of the limbs and face, hypotonia, and
696 developmental delay. Am. J. Hum. Genet. **96**: 462–473.

697 Coleman D. E., Berghuis A. M., Lee E., Linder M. E., Gilman A. G., Sprang S. R., 1994 Structures of active
698 conformations of Gi alpha 1 and the mechanism of GTP hydrolysis. Science **265**: 1405–1412.

699 Coulon P., Kanyshkova T., Broicher T., Munsch T., Wettschureck N., Seidenbecher T., Meuth S. G.,
700 Offermanns S., Pape H.-C., Budde T., 2010 Activity Modes in Thalamocortical Relay Neurons are
701 Modulated by G(q)/G(11) Family G-proteins - Serotonergic and Glutamatergic Signaling. Front Cell
702 Neurosci **4**: 132.

703 Davis M. W., Hammarlund M., Harrach T., Hullett P., Olsen S., Jorgensen E. M., 2005 Rapid single
704 nucleotide polymorphism mapping in C. elegans. BMC Genomics **6**: 118.

705 Davis M. W., Morton J. J., Carroll D., Jorgensen E. M., 2008 Gene activation using FLP recombinase in C.
706 elegans. PLoS Genet. **4**: e1000028.

707 Esposito G., Amoroso M. R., Bergamasco C., Di Schiavi E., Bazzicalupo P., 2010 The G protein regulators
708 EGL-10 and EAT-16, the Giα GOA-1 and the G(q)α EGL-30 modulate the response of the C.
709 elegans ASH polymodal nociceptive sensory neurons to repellents. BMC Biol. **8**: 138.

710 Etienne-Manneville S., Hall A., 2002 Rho GTPases in cell biology. Nature **420**: 629–635.

711 Fukai R., Saitsu H., Okamoto N., Sakai Y., Fattal-Valevski A., Masaaki S., Kitai Y., Torio M., Kojima-Ishii
712 K., Ihara K., Chernuha V., Nakashima M., Miyatake S., Tanaka F., Miyake N., Matsumoto N., 2016
713 De novo missense mutations in NALCN cause developmental and intellectual impairment with
714 hypotonia. J. Hum. Genet. **61**: 451–455.

715 Funato H., Miyoshi C., Fujiyama T., Kanda T., Sato M., Wang Z., Ma J., Nakane S., Tomita J., Ikkyu A.,
716 Kakizaki M., Hotta-Hirashima N., Kanno S., Komiya H., Asano F., Honda T., Kim S. J., Harano K.,
717 Muramoto H., Yonezawa T., Mizuno S., Miyazaki S., Connor L., Kumar V., Miura I., Suzuki T.,
718 Watanabe A., Abe M., Sugiyama F., Takahashi S., Sakimura K., Hayashi Y., Liu Q., Kume K.,
719 Wakana S., Takahashi J. S., Yanagisawa M., 2016 Forward-genetics analysis of sleep in randomly
720 mutagenized mice. Nature **539**: 378–383.

721 Gal M., Magen D., Zahran Y., Ravid S., Eran A., Khayat M., Gafni C., Levanon E. Y., Mandel H., 2016 A
722 novel homozygous splice site mutation in NALCN identified in siblings with cachexia, strabismus,
723 severe intellectual disability, epilepsy and abnormal respiratory rhythm. Eur J Med Genet **59**: 204–
724 209.

725 Gamper N., Reznikov V., Yamada Y., Yang J., Shapiro M. S., 2004 Phosphatidylinositol [correction] 4,5-
726 bisphosphate signals underlie receptor-specific Gq/11-mediated modulation of N-type Ca2+
727 channels. J. Neurosci. **24**: 10980–10992.

728 Gao S., Xie L., Kawano T., Po M. D., Pirri J. K., Guan S., Alkema M. J., Zhen M., 2015 The NCA sodium
729 leak channel is required for persistent motor circuit activity that sustains locomotion. Nat Commun
730 **6**: 6323.

731 Hajdu-Cronin Y. M., Chen W. J., Patikoglou G., Koelle M. R., Sternberg P. W., 1999 Antagonism between
732 G(o)alpha and G(q)alpha in Caenorhabditis elegans: the RGS protein EAT-16 is necessary for
733 G(o)alpha signaling and regulates G(q)alpha activity. Genes Dev **13**: 1780–1793.

734 Hajdu-Cronin Y. M., Chen W. J., Sternberg P. W., 2004 The L-type cyclin CYL-1 and the heat-shock-factor
735 HSF-1 are required for heat-shock-induced protein expression in Caenorhabditis elegans. Genetics
736 **168**: 1937–1949.

737 Hammarlund M., Palfreyman M. T., Watanabe S., Olsen S., Jorgensen E. M., 2007 Open syntaxin docks
738 synaptic vesicles. PLoS Biol. **5**: e198.

739 Hiley E., McMullan R., Nurrish S. J., 2006 The Galpha12-RGS RhoGEF-RhoA signalling pathway regulates
740 neurotransmitter release in C. elegans. EMBO J. **25**: 5884–5895.

741 Humphrey J. A., Hamming K. S., Thacker C. M., Scott R. L., Sedensky M. M., Snutch T. P., Morgan P. G.,
742 Nash H. A., 2007 A putative cation channel and its novel regulator: cross-species conservation of
743 effects on general anesthesia. Curr. Biol. **17**: 624–629.

744 Jaffe A. B., Hall A., 2005 Rho GTPases: biochemistry and biology. Annu. Rev. Cell Dev. Biol. **21**: 247–269.

745 Jantsch-Plunger V., Gönczy P., Romano A., Schnabel H., Hamill D., Schnabel R., Hyman A. A., Glotzer M.,
746 2000 CYK-4: A Rho family gtpase activating protein (GAP) required for central spindle formation
747 and cytokinesis. J. Cell Biol. **149**: 1391–1404.

748 Jospin M., Watanabe S., Joshi D., Young S., Hamming K., Thacker C., Snutch T. P., Jorgensen E. M.,
749 Schuske K., 2007 UNC-80 and the NCA ion channels contribute to endocytosis defects in
750 synaptojanin mutants. Curr. Biol. **17**: 1595–1600.

751 Karakaya M., Heller R., Kunde V., Zimmer K.-P., Chao C.-M., Nürnberg P., Cirak S., 2016 Novel Mutations
752 in the Nonselective Sodium Leak Channel (NALCN) Lead to Distal Arthrogryposis with Increased
753 Muscle Tone. Neuropediatrics **47**:273-277.

754 Köroğlu Ç., Seven M., Tolun A., 2013 Recessive truncating NALCN mutation in infantile neuroaxonal
755 dystrophy with facial dysmorphism. J. Med. Genet. **50**: 515–520.

756 Krause M., Offermanns S., Stocker M., Pedarzani P., 2002 Functional specificity of G alpha q and G alpha
757 11 in the cholinergic and glutamatergic modulation of potassium currents and excitability in
758 hippocampal neurons. J. Neurosci. **22**: 666–673.

759 Lackner M. R., Nurrish S. J., Kaplan J. M., 1999 Facilitation of synaptic transmission by EGL-30 Gqalpha
760 and EGL-8 PLCbeta: DAG binding to UNC-13 is required to stimulate acetylcholine release. Neuron
761 **24**: 335–346.

762 Lear B. C., Lin J.-M., Keath J. R., McGill J. J., Raman I. M., Allada R., 2005 The ion channel narrow
763 abdomen is critical for neural output of the Drosophila circadian pacemaker. Neuron **48**: 965–976.

764 Lear B. C., Darrah E. J., Aldrich B. T., Gebre S., Scott R. L., Nash H. A., Allada R., 2013 UNC79 and
765 UNC80, Putative Auxiliary Subunits of the NARROW ABDOMEN Ion Channel, Are Indispensable
766 for Robust Circadian Locomotor Rhythms in Drosophila. PLoS ONE **8**: e78147.

767 Lee J. H., Cribbs L. L., Perez-Reyes E., 1999 Cloning of a novel four repeat protein related to voltage-
768 gated sodium and calcium channels. FEBS Lett. **445**: 231–236.

769 Liebeskind B. J., Hillis D. M., Zakon H. H., 2012 Phylogeny unites animal sodium leak channels with fungal
770 calcium channels in an ancient, voltage-insensitive clade. Mol. Biol. Evol. **29**: 3613–3616.

771 Littleton J. T., Ganetzky B., 2000 Ion channels and synaptic organization: analysis of the Drosophila
772 genome. Neuron **26**: 35–43.

773 Lu B., Su Y., Das S., Liu J., Xia J., Ren D., 2007 The neuronal channel NALCN contributes resting sodium
774 permeability and is required for normal respiratory rhythm. Cell **129**: 371–383.

775 Lu B., Su Y., Das S., Wang H., Wang Y., Liu J., Ren D., 2009 Peptide neurotransmitters activate a cation
776 channel complex of NALCN and UNC-80. Nature **457**: 741–744.

777 Lu B., Zhang Q., Wang H., Wang Y., Nakayama M., Ren D., 2010 Extracellular calcium controls
778 background current and neuronal excitability via an UNC79-UNC80-NALCN cation channel
779 complex. Neuron **68**: 488–499.

780 Lu T. Z., Feng Z.-P., 2011 A sodium leak current regulates pacemaker activity of adult central pattern
781 generator neurons in Lymnaea stagnalis. PLoS ONE **6**: e18745.

782 Lutas A., Lahmann C., Soumillon M., Yellen G., 2016 The leak channel NALCN controls tonic firing and
783 glycolytic sensitivity of substantia nigra pars reticulata neurons. eLife **5**: e15271.

784 Lutz S., Freichel-Blomquist A., Yang Y., Rümenapp U., Jakobs K. H., Schmidt M., Wieland T., 2005 The
785 guanine nucleotide exchange factor p63RhoGEF, a specific link between Gq/11-coupled receptor
786 signaling and RhoA. J. Biol. Chem. **280**: 11134–11139.

787 Lutz S., Shankaranarayanan A., Coco C., Ridilla M., Nance M. R., Vettel C., Baltus D., Evelyn C. R.,
788 Neubig R. R., Wieland T., Tesmer J. J. G., 2007 Structure of Galphaq-p63RhoGEF-RhoA complex
789 reveals a pathway for the activation of RhoA by GPCRs. Science **318**: 1923–1927.

790 Matsuki M., Kunitomo H., Iino Y., 2006 Goalpha regulates olfactory adaptation by antagonizing Gqalpha-
791 DAG signaling in Caenorhabditis elegans. Proc. Natl. Acad. Sci. U.S.A. **103**: 1112–1117.

792 McMullan R., Hiley E., Morrison P., Nurrish S. J., 2006 Rho is a presynaptic activator of neurotransmitter
793 release at pre-existing synapses in C. elegans. Genes Dev. **20**: 65–76.

794 Mello C. C., Kramer J. M., Stinchcomb D., Ambros V., 1991 Efficient gene transfer in C.elegans:
795 extrachromosomal maintenance and integration of transforming sequences. EMBO J **10**: 3959–
796 3970.

797 Miller K. G., Emerson M. D., Rand J. B., 1999 Goalpha and diacylglycerol kinase negatively regulate the
798 Gqalpha pathway in C. elegans. Neuron **24**: 323–333.

799 Park E. C., Horvitz H. R., 1986 Mutations with dominant effects on the behavior and morphology of the
800 nematode Caenorhabditis elegans. Genetics **113**: 821–852.

801 Pereira L., Kratsios P., Serrano-Saiz E., Sheftel H., Mayo A. E., Hall D. H., White J. G., LeBoeuf B., Garcia
802 L. R., Alon U., Hobert O., 2015 A cellular and regulatory map of the cholinergic nervous system of
803 C. elegans. eLife **4**: e12432.

804 Perez Y., Kadir R., Volodarsky M., Noyman I., Flusser H., Shorer Z., Gradstein L., Birnbaum R. Y., Birk O.
805 S., 2016 UNC80 mutation causes a syndrome of hypotonia, severe intellectual disability, dyskinesia
806 and dysmorphism, similar to that caused by mutations in its interacting cation channel NALCN. J.
807 Med. Genet. **53**: 397–402.

808 Pierce-Shimomura J. T., Chen B. L., Mun J. J., Ho R., Sarkis R., McIntire S. L., 2008 Genetic analysis of
809 crawling and swimming locomotory patterns in C. elegans. Proc. Natl. Acad. Sci. U.S.A. **105**:
810 20982–20987.

811 Sánchez-Fernández G., Cabezudo S., García-Hoz C., Benincá C., Aragay A. M., Mayor F., Ribas C., 2014
812 Gαq signalling: the new and the old. Cell. Signal. **26**: 833–848.

813 Senatore A., Monteil A., Minnen J. van, Smit A. B., Spafford J. D., 2013 NALCN ion channels have
814 alternative selectivity filters resembling calcium channels or sodium channels. PLoS ONE **8**:
815 e55088.

816 Senatore A., Spafford J. D., 2013 A uniquely adaptable pore is consistent with NALCN being an ion sensor.
817 Channels (Austin) **7**: 60–68.

818 Shamseldin H. E., Faqeih E., Alasmari A., Zaki M. S., Gleeson J. G., Alkuraya F. S., 2016 Mutations in
819 UNC80, Encoding Part of the UNC79-UNC80-NALCN Channel Complex, Cause Autosomal-
820 Recessive Severe Infantile Encephalopathy. Am. J. Hum. Genet. **98**: 210–215.

821 Stray-Pedersen A., Cobben J.-M., Prescott T. E., Lee S., Cang C., Aranda K., Ahmed S., Alders M.,
822 Gerstner T., Aslaksen K., Tétreault M., Qin W., Hartley T., Jhangiani S. N., Muzny D. M., Tarailo-

823 Graovac M., Karnebeek C. D. M. van, Care4Rare Canada Consortium, Baylor-Hopkins Center for
824 Mendelian Genomics, Lupski J. R., Ren D., Yoon G., 2016 Biallelic Mutations in UNC80 Cause
825 Persistent Hypotonia, Encephalopathy, Growth Retardation, and Severe Intellectual Disability. Am.
826 J. Hum. Genet. **98**: 202–209.

827 Swayne L. A., Mezghrani A., Varrault A., Chemin J., Bertrand G., Dalle S., Bourinet E., Lory P., Miller R. J.,
828 Nargeot J., Monteil A., 2009 The NALCN ion channel is activated by M3 muscarinic receptors in a
829 pancreatic beta-cell line. EMBO Rep. **10**: 873–880.

830 Topalidou I., Cattin-Ortolá J., Pappas A. L., Cooper K., Merrihew G. E., MacCoss M. J., Ailion M., 2016 The
831 EARP Complex and Its Interactor EIPR-1 Are Required for Cargo Sorting to Dense-Core Vesicles.
832 PLoS Genet. **12**: e1006074.

833 Vogt S., Grosse R., Schultz G., Offermanns S., 2003 Receptor-dependent RhoA activation in G12/G13-
834 deficient cells: genetic evidence for an involvement of Gq/G11. J. Biol. Chem. **278**: 28743–28749.

835 Wang Y., Koh K., Ichinose Y., Yasumura M., Ohtsuka T., Takiyama Y., 2016 A de novo mutation in the
836 NALCN gene in an adult patient with cerebellar ataxia associated with intellectual disability and
837 arthrogryposis. Clin. Genet. **90**: 556–557.

838 Weernink P. A. O., Meletiadis K., Hommeltenberg S., Hinz M., Ishihara H., Schmidt M., Jakobs K. H., 2004
839 Activation of type I phosphatidylinositol 4-phosphate 5-kinase isoforms by the Rho GTPases, RhoA,
840 Rac1, and Cdc42. J. Biol. Chem. **279**: 7840–7849.

841 Wilkie T. M., Scherle P. A., Strathmann M. P., Slepak V. Z., Simon M. I., 1991 Characterization of G-
842 protein alpha subunits in the Gq class: expression in murine tissues and in stromal and
843 hematopoietic cell lines. Proc. Natl. Acad. Sci. U.S.A. **88**: 10049–10053.

844 Wilkie T. M., Gilbert D. J., Olsen A. S., Chen X. N., Amatruda T. T., Korenberg J. R., Trask B. J., Jong P.
845 de, Reed R. R., Simon M. I., 1992 Evolution of the mammalian G protein alpha subunit multigene
846 family. Nat. Genet. **1**: 85–91.

847 Williams S. L., Lutz S., Charlie N. K., Vettel C., Ailion M., Coco C., Tesmer J. J. G., Jorgensen E. M.,
848 Wieland T., Miller K. G., 2007 Trio's Rho-specific GEF domain is the missing Galpha q effector in C.
849 elegans. Genes Dev **21**: 2731–2746.

850 Xie L., Gao S., Alcaire S. M., Aoyagi K., Wang Y., Griffin J. K., Stagljar I., Nagamatsu S., Zhen M., 2013
851 NLF-1 delivers a sodium leak channel to regulate neuronal excitability and modulate rhythmic
852 locomotion. Neuron **77**: 1069–1082.

853 Yeh E., Ng S., Zhang M., Bouhours M., Wang Y., Wang M., Hung W., Aoyagi K., Melnik-Martinez K., Li M.,
854 Liu F., Schafer W. R., Zhen M., 2008 A putative cation channel, NCA-1, and a novel protein, UNC-
855 80, transmit neuronal activity in C. elegans. PLoS Biol. **6**: e55.

856

Figure 1

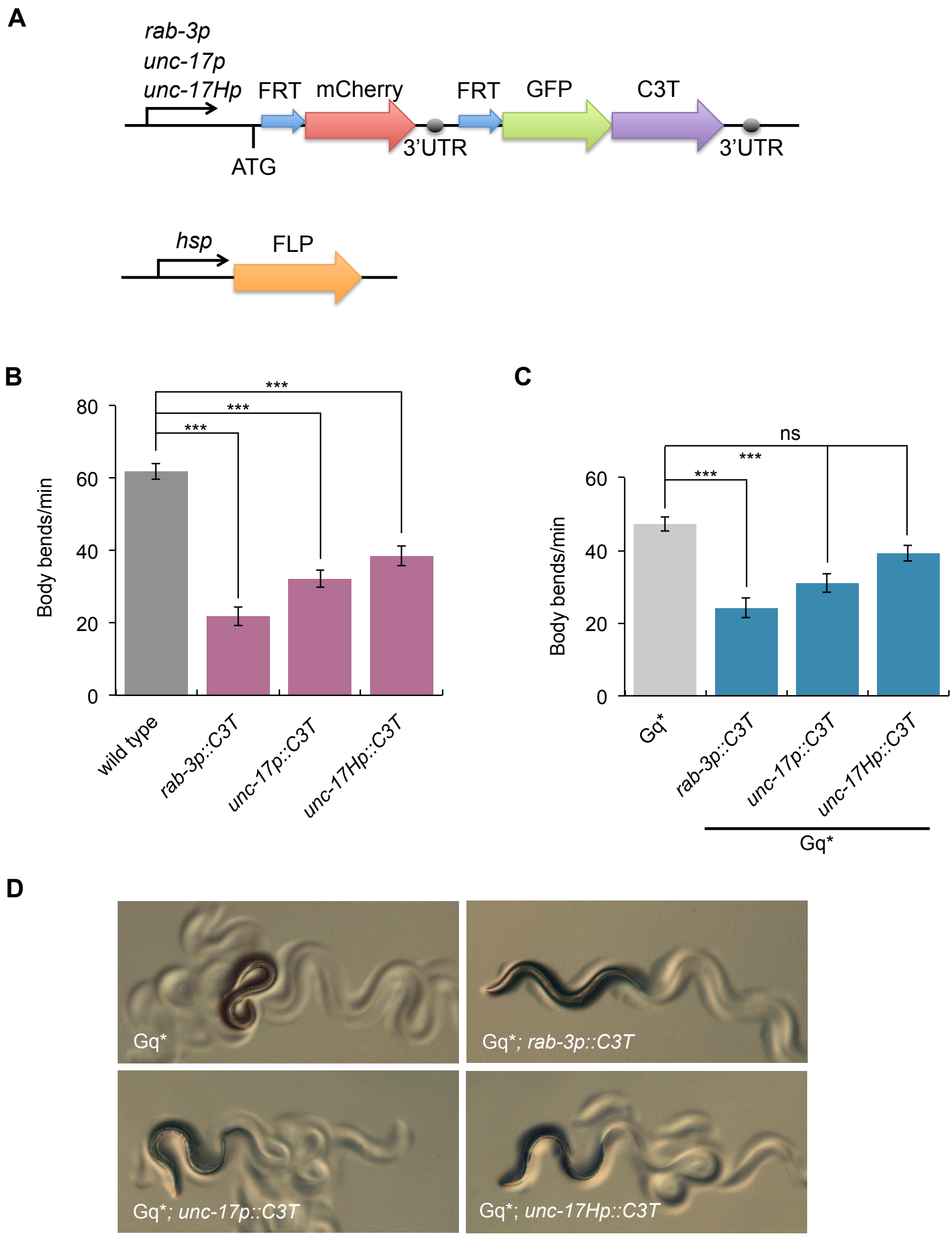
A
rab-3p
unc-17p
unc-17Hp
FRT
mCherry
FRT
GFP
C3T
ATG
3'UTR
3'UTR
hsp
FLP
B
Body bends/min
80
60
40
20
0
***
***
***
wild type
rab-3p::C3T
unc-17p::C3T
unc-17Hp::C3T
C
Body bends/min
60
40
20
0
ns
***
***
Gq*
rab-3p::C3T
unc-17p::C3T
unc-17Hp::C3T
Gq*
D
Gq*
Gq*; rab-3p::C3T
Gq*; unc-17p::C3T
Gq*; unc-17Hp::C3T

Figure 2

A

WT
Nca*
Nca*; *nlf-1*

B

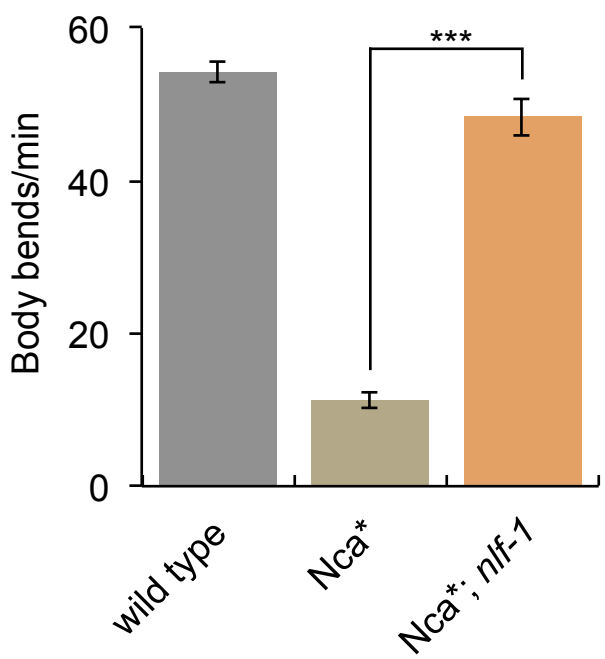
Body bends/min
60
40
20
0
***
wild type
Nca*
Nca*; *nlf-1*

C

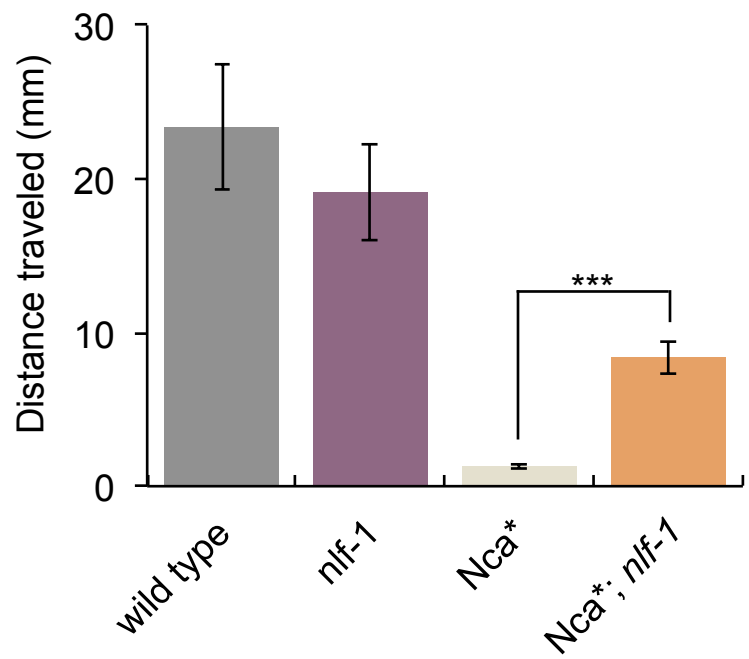
Distance traveled (mm)
30
20
10
0
***
wild type
nlf-1
Nca*
Nca*; *nlf-1*

Figure 3

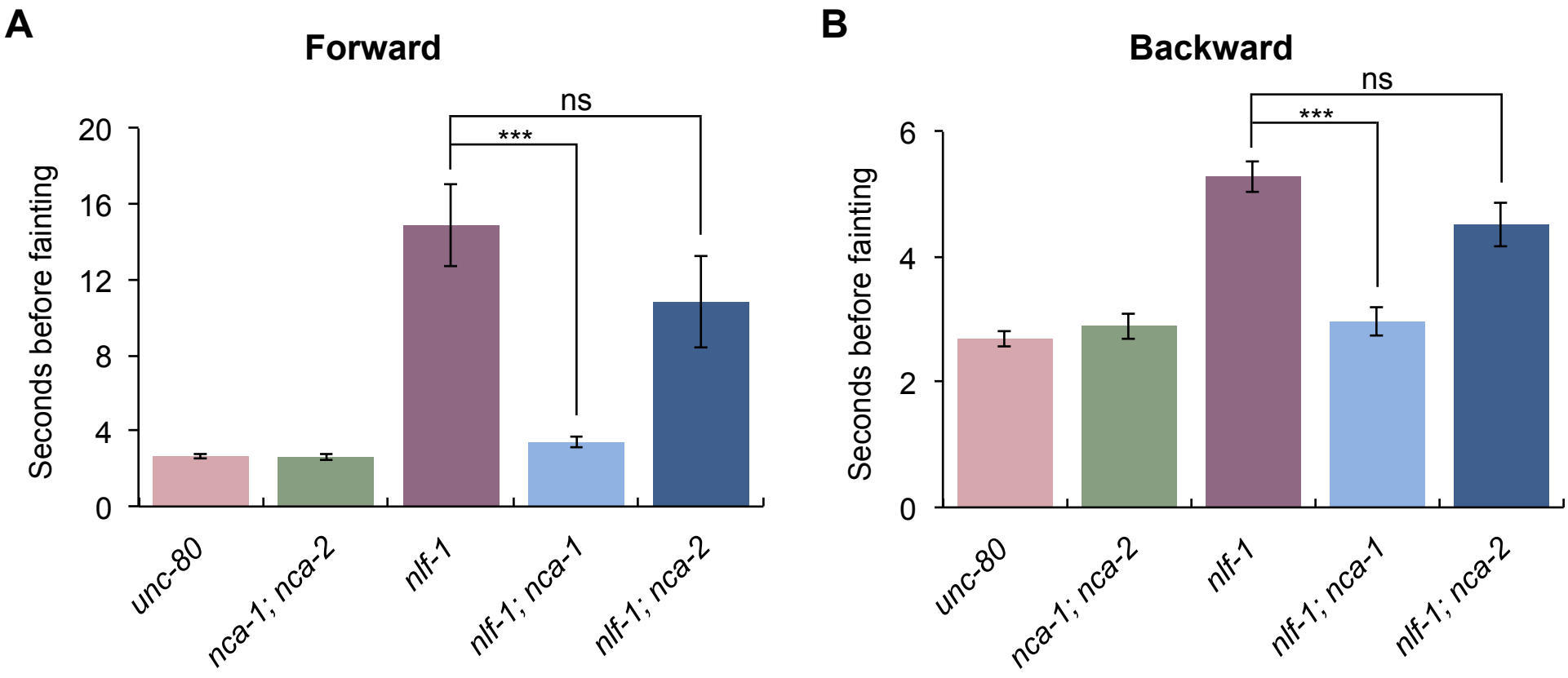
A
Forward
Seconds before fainting
20
16
12
8
4
0
ns
***
unc-80
nca-1; nca-2
nlf-1
nlf-1; nca-1
nlf-1; nca-2
B
Backward
Seconds before fainting
6
4
2
0
ns
***
unc-80
nca-1; nca-2
nlf-1
nlf-1; nca-1
nlf-1; nca-2

Figure 4

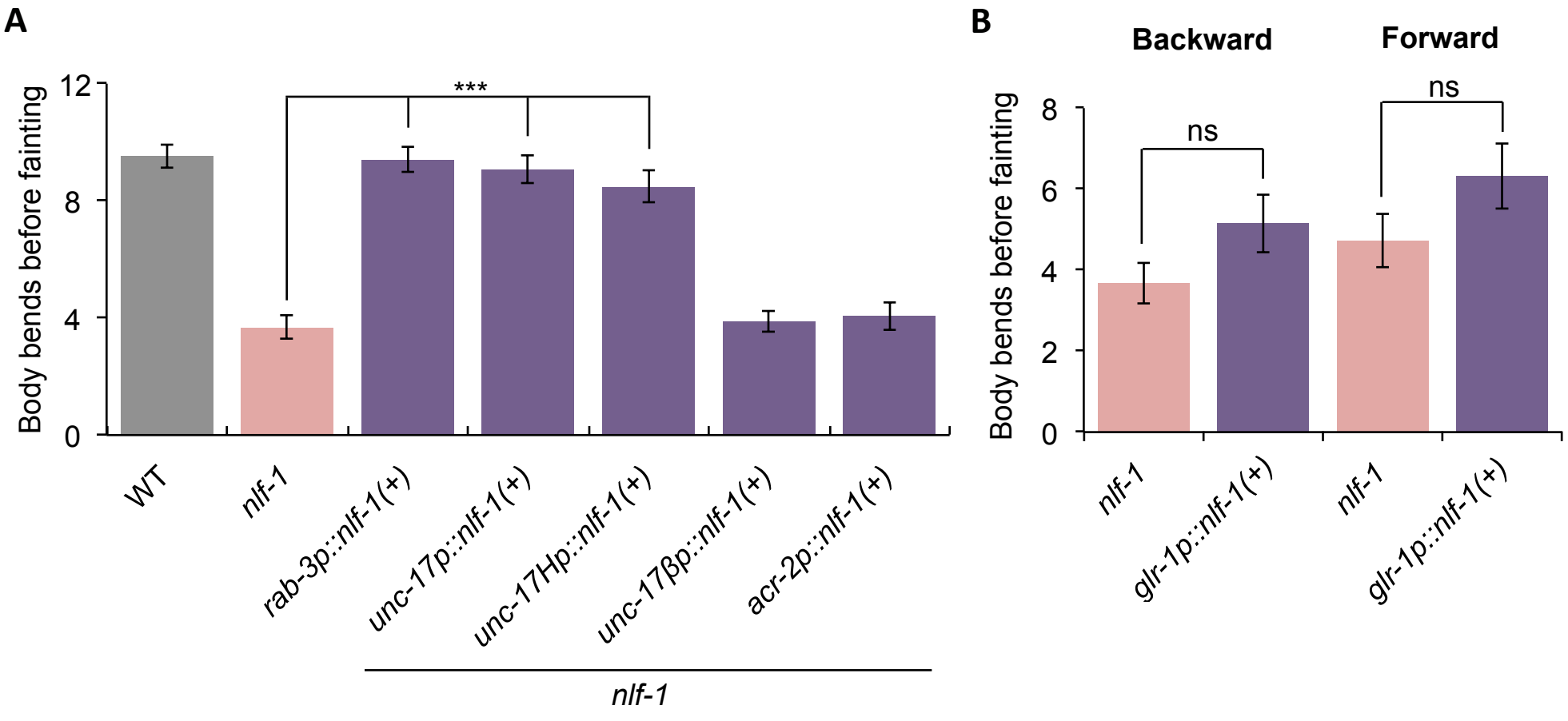
A
Body bends before fainting
12
8
4
0
***
WT
nlf-1
rab-3p::nlf-1(+)
unc-17p::nlf-1(+)
unc-17Hp::nlf-1(+)
unc-17βp::nlf-1(+)
acr-2p::nlf-1(+)
nlf-1
B
Backward
Forward
Body bends before fainting
8
6
4
2
0
ns
ns
nlf-1
glr-1p::nlf-1(+)
nlf-1
glr-1p::nlf-1(+)

Figure 5

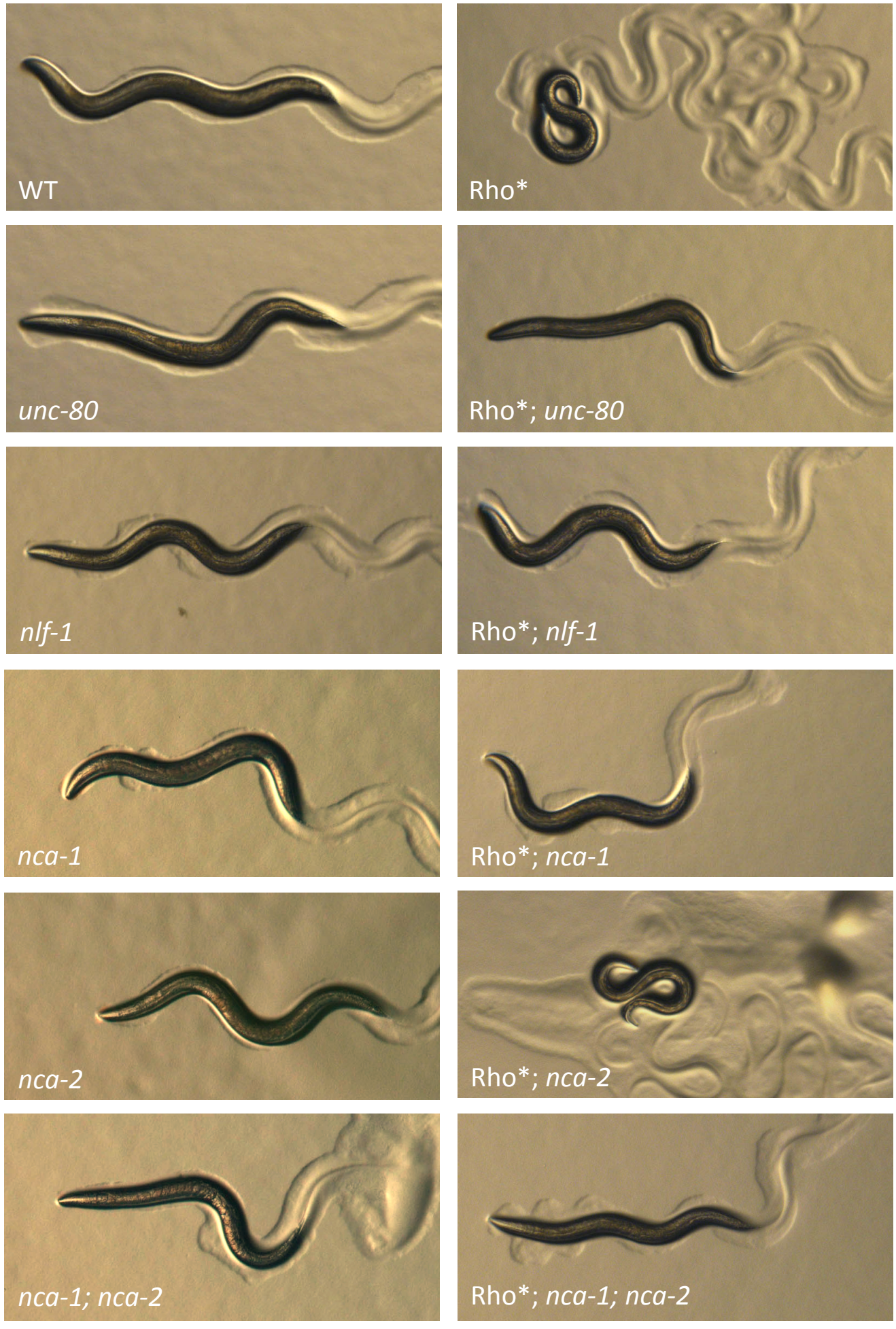
WT
Rho*
unc-80
Rho*; unc-80
nlf-1
Rho*; nlf-1
nca-1
Rho*; nca-1
nca-2
Rho*; nca-2
nca-1; nca-2
Rho*; nca-1; nca-2

Figure 6

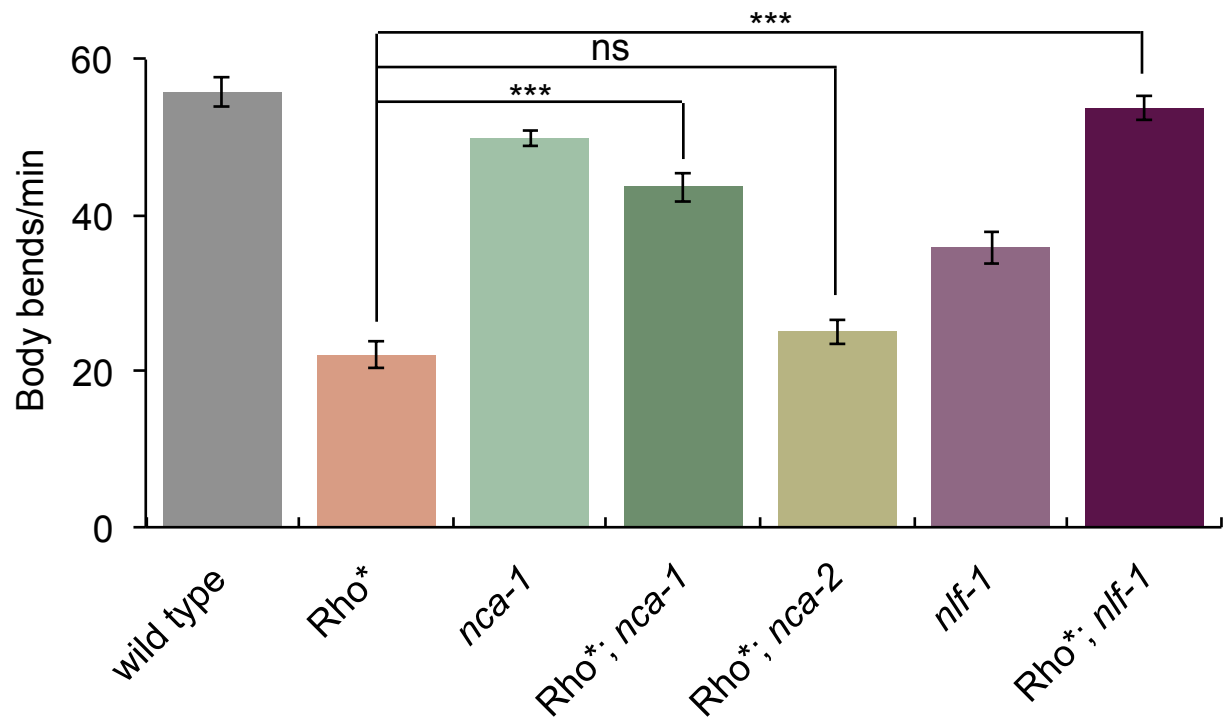
***
ns
***
60
40
20
0
Body bends/min
wild type
Rho*
nca-1
Rho*; nca-1
Rho*; nca-2
nlf-1
Rho*; nlf-1

Figure 7

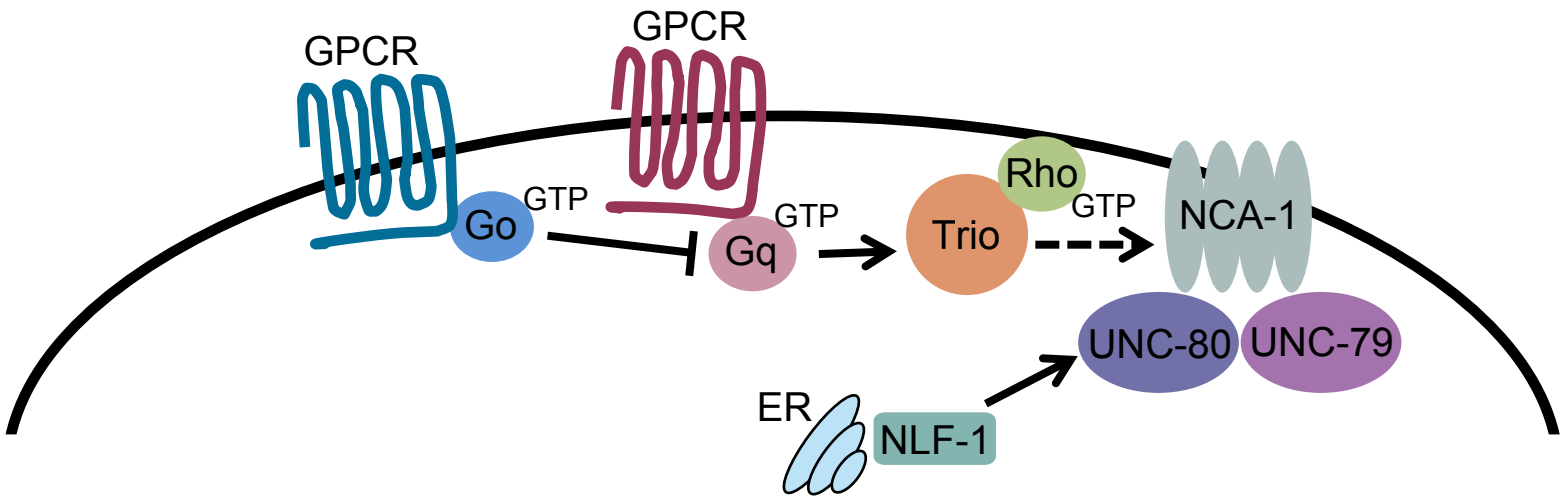

Figure S1

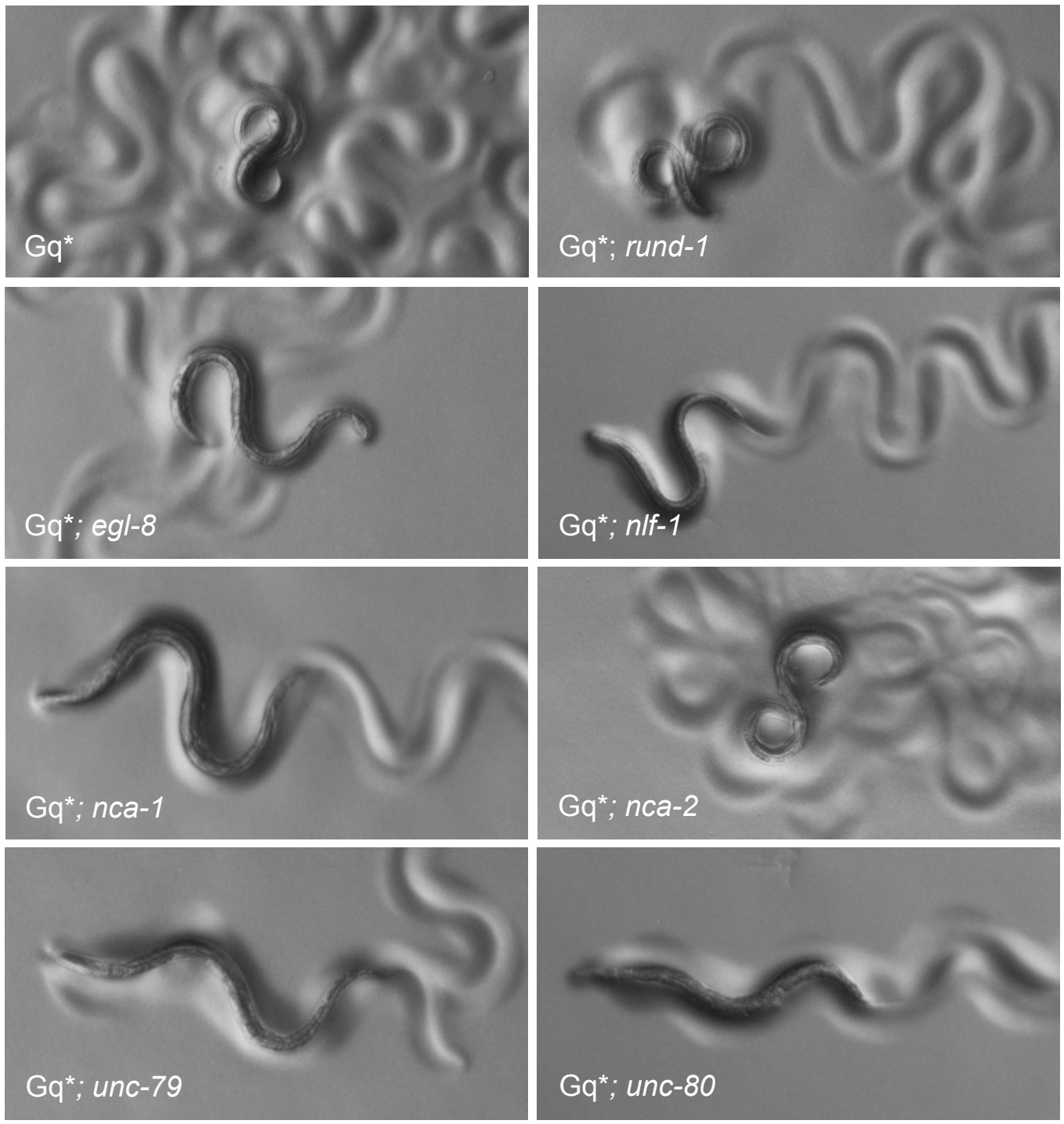

Figure S2

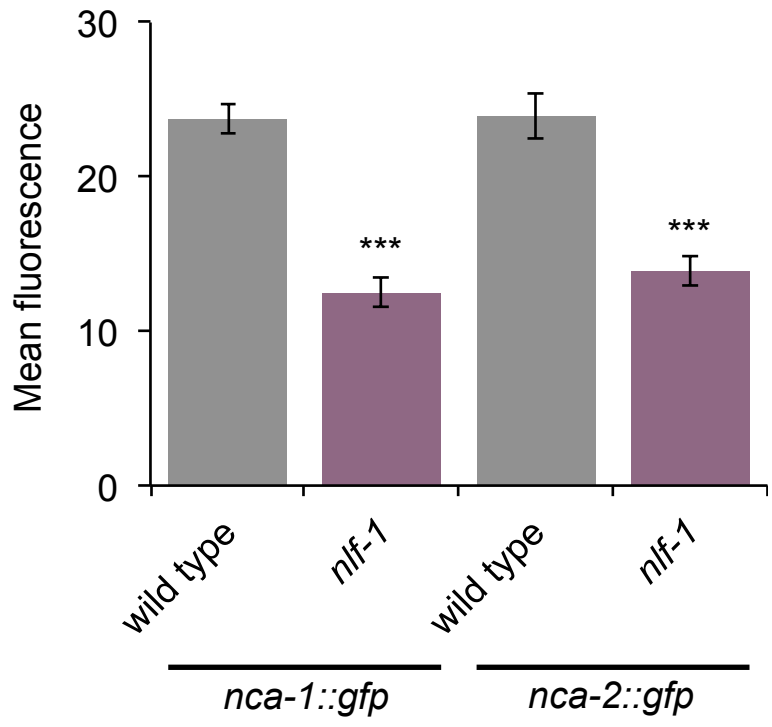
30
20
10
0
Mean fluorescence
***
***
wild type
nlf-1
wild type
nlf-1
nca-1::gfp
nca-2::gfp

Figure S3

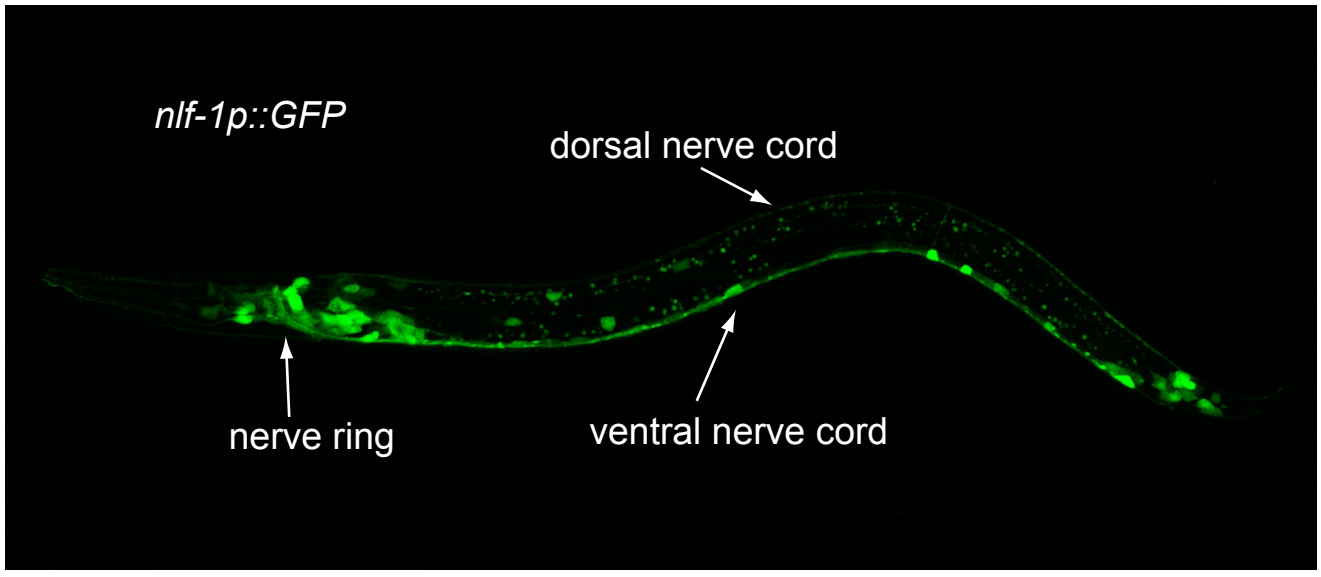

Figure S4

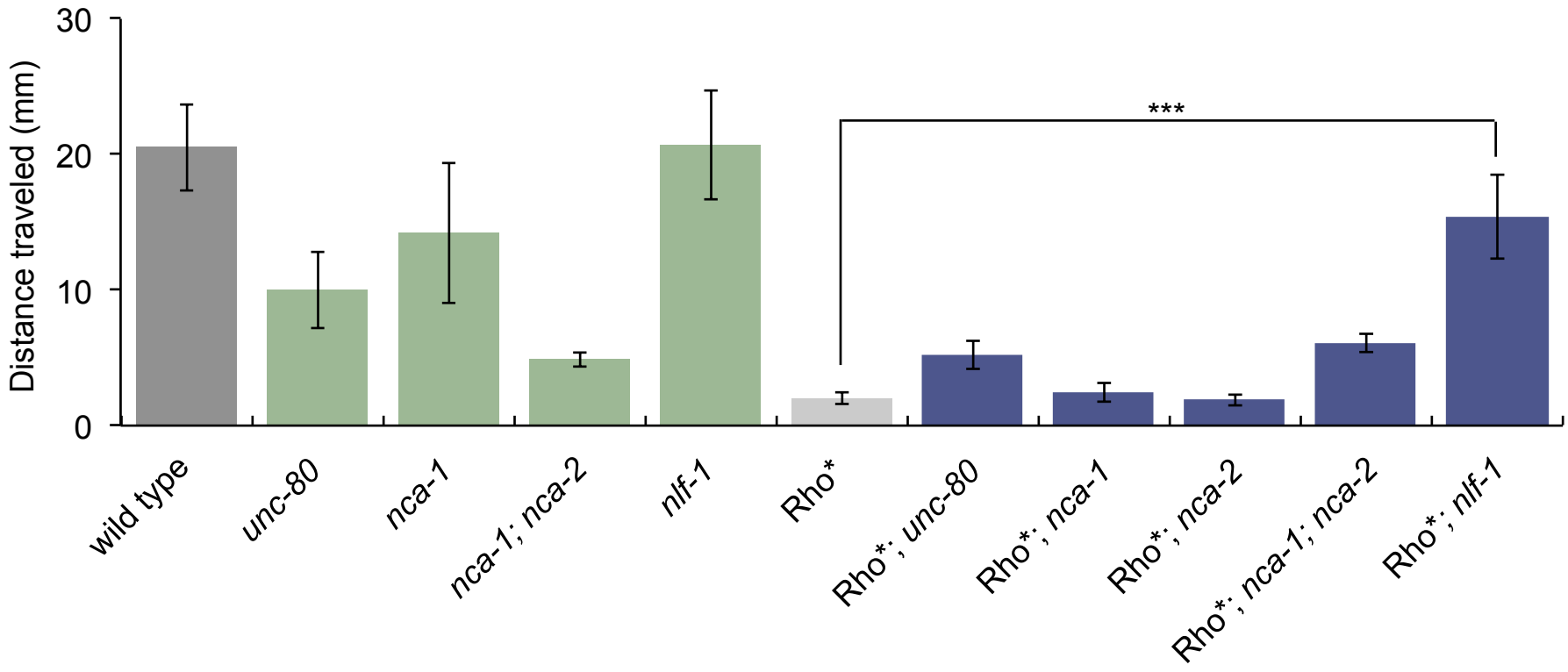
Distance traveled (mm)
30
20
10
0
***
wild type
unc-80
nca-1
nca-1; nca-2
nlf-1
Rho*
Rho*; unc-80
Rho*; nca-1
Rho*; nca-2
Rho*; nca-1; nca-2
Rho*; nlf-1

Figure S5

A

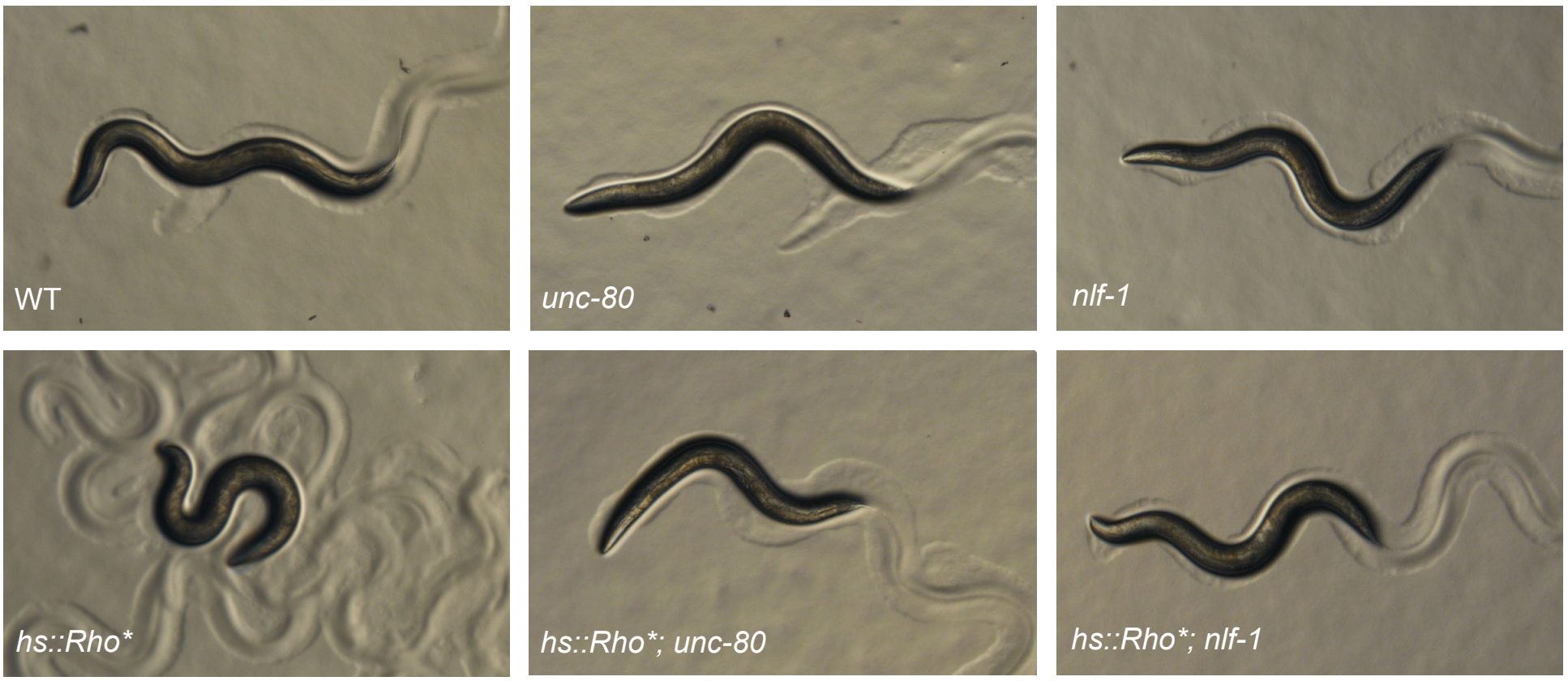
WT
unc-80
nlf-1
hs::Rho*
hs::Rho*; unc-80
hs::Rho*; nlf-1

B

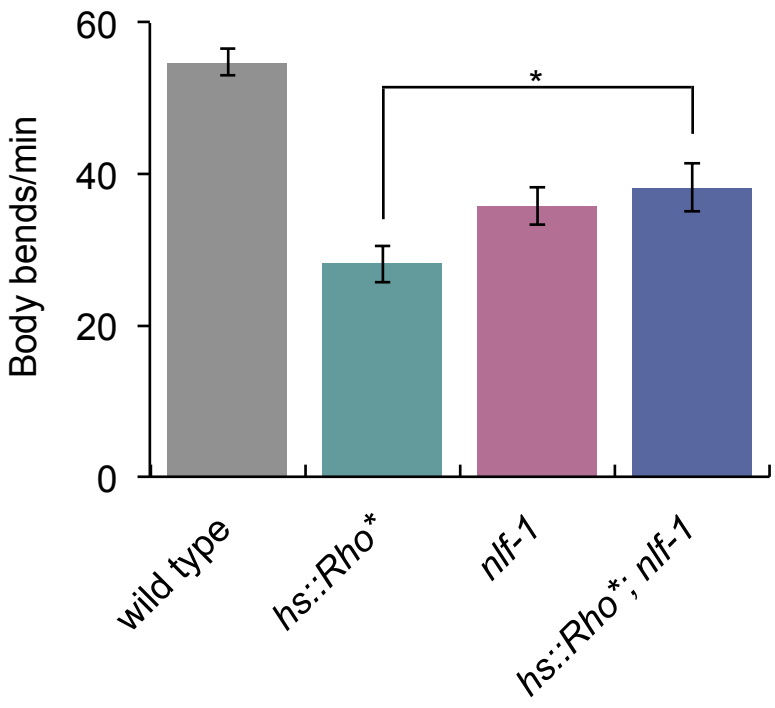
60
40
20
0
Body bends/min
*
wild type
hs::Rho*
nlf-1
hs::Rho*; nlf-1

Table S1. List of strains

CB4856 Hawaiian wild isolate
EG303 *goa-1(n499 ox303) I*
EG304 *goa-1(n499 ox304) I*
EG327 *nlf-1(ox327) X*
EG330 *unc-80(ox330) V*
EG352 *nca-1(ox352) IV*
EG3447 *egl-30(tg26) I goa-1(n499) I / egl-30(tg26) I goa-1(+) I*
EG3498 *egl-30(tg26) I goa-1(n499) I / egl-30(tg26) I unc-13(e51) I gld-1(q126) I*
EG3647 *egl-30(tg26) I ; nlf-1(ox327) X*
EG3649 *egl-30(tg26) I ; unc-80(ox329) V*
EG3650 *egl-30(tg26) I ; unc-80(ox330) V*
EG3761 *unc-79(e1068) III*
EG3771 *egl-30(tg26) I ; unc-80(e1272) V*
EG3798 *egl-30(tg26) I ; egl-8(ox333) V*
EG3804 *nca-2(gk5) III ; nca-1(gk9) IV*
EG4036 *egl-30(tg26) I ; nca-2(gk5) III ; nca-1(gk9) IV*
EG4067 *goa-1(n499 ox304) I; nca-1(ox352) IV*
EG4494 *nca-1(ox352) IV ; nlf-1(ox327) X*
EG4530 *nzIs29[unc-17p::rho-1(G14V), unc-122p::gfp] II ; unc-79(e1068) III*
EG4531 *nzIs29[unc-17p::rho-1(G14V), unc-122p::gfp] II ; unc-80(ox330) V*
EG4532 *egl-30(tg26) I*
EG4681 *nzIs29[unc-17p::rho-1(G14V), unc-122p::gfp] II ; nlf-1(ox327) X*
EG4684 *nzIs1[hs::rho-1(G14V), ttx-3p::gfp] I ; unc-79(e1068) III*
EG4685 *nzIs1[hs::rho-1(G14V), ttx-3p::gfp] I ; unc-80(ox330) V*
EG4686 *nzIs1[hs::rho-1(G14V), ttx-3p::gfp] I ; nlf-1(ox327) X*
EG4690 *nzIs29[unc-17p::rho-1(G14V), unc-122p::gfp] II ; nca-2(gk5) III ; nca-1(gk9) IV*
EG4694 *unc-80(ox330) V ; nlf-1(ox327) X*
EG4697 *unc-79(e1068) III ; nlf-1(ox327) X*
EG4700 *nzIs29[unc-17p::rho-1(G14V), unc-122p::gfp] II ; nca-1(gk9) IV*
EG4718 *nlf-1(ox327) X ; oxEx1041[cosmid F55A4, unc-17p::mCherry::H2B, lin-15(+)]*
EG4733 *nca-1(gk9) IV ; vaIs46[NCA-1::GFP, lin-15+] X*
EG4761 *nzIs29[unc-17p::rho-1(G14V), unc-122p::gfp] II ; nca-2(gk5) III*
EG4782 *nzIs29[unc-17p::rho-1(G14V), unc-122p::gfp] II*
EG4783 *nca-2(gk5) III ; vaIs41[NCA-2::GFP, lin-15+]*
EG4785 *egl-30(tg26) I ; nca-1(gk9) IV*
EG4786 *egl-30(tg26) I ; nca-2(gk5) III*
EG4834 *nca-1(gk9) IV; nlf-1(ox327) X*
EG4835 *nca-2(gk5) IV; nlf-1(ox327) X*
EG4836 *nlf-1(ox327) X ; vaIs46[NCA-1::GFP, lin-15+]*
EG4837 *nlf-1(ox327) X ; vaIs41[NCA-2::GFP, lin-15+]*
EG4943 *nlf-1(ox327) X ; oxEx1146[rab-3p::nlf-1(+) cDNA::GFP, myo-2p::mCherry]*
EG5217 *oxIs412[rab-3p-FRT-mCherry-FRT-GFP-C3T, lin-15(+), hsp-FLP] II*
EG5218 *oxIs414[unc-17p-FRT-mCherry-FRT-GFP-C3T, lin-15(+), hsp-FLP] II*
EG5252 *egl-30(tg26) I ; oxIs412[rab-3p-FRT-mCherry-FRT-GFP-C3T, lin-15(+), hsp-FLP] II*
EG5263 *egl-30(tg26) I ; oxIs414[unc-17p-FRT-mCherry-FRT-GFP-C3T, lin-15(+), hsp-FLP] II*
EG5279 *oxIs434[unc-17Hp-FRT-mCherry-FRT-GFP-C3T, lin-15(+), hsp-FLP] X*
EG5287 *egl-30(tg26) I ; oxIs434[unc-17Hp-FRT-mCherry-FRT-GFP-C3T, lin-15(+), hsp-FLP] X*
EG5320 *oxIs435[unc-17βp-FRT-mCherry-FRT-GFP-C3T, lin-15(+), hsp-FLP] II*
EG5504 *nlf-1(tm3631) X*
EG5609 *egl-30(tg26) I ; rund-1(tm3622) X*

EG5611 *egl-30(tg26) I ; nlf-1(tm3631) X*
EG7249 *eri-1(mg366) IV ; lin-15(n744) X*
MT1102 *goa-1(n499) I / +*
N2 Bristol isolate, standard lab wild type
QT47 *nzIs1[hs::rho-1(G14V), ttx-3p::gfp] I*
VC9 *nca-2(gk5) III*
VC12 *nca-1(gk9) IV*
XZ1080 *egl-30(tg26) I ; unc-80(yak8) V*
XZ1113 *egl-30(tg26) I ; unc-80(yak35) V*
XZ1114 *egl-30(tg26) I ; unc-80(yak36) V*
XZ1115 *egl-30(tg26) I ; unc-79(yak37) III*
XZ1151 *egl-30(tg26) I*
XZ1152 *egl-30(tg26) I ; nuIs183[unc-129p::NLP-21-Venus, myo-2p::NLS-GFP] III*
XZ1186 *egl-30(tg26) I ; nuIs183[unc-129p::NLP-21-Venus, myo-2p::NLS-GFP] III; unc-80(yak56) V*
XZ1191 *egl-30(tg26) I ; unc-79(yak61) III nuIs183[unc-129p::NLP-21-Venus, myo-2p::NLS-GFP] III*
XZ1229 *egl-30(tg26) I ; unc-79(yak73) III nuIs183[unc-129p::NLP-21-Venus, myo-2p::NLS-GFP] III*
XZ2008 *lin-15(n765ts) X ; oxEx1144[nlf-1p::GFP, lin-15(+)]*
XZ2009 *nlf-1(ox327) X ; oxEx1147[nlf-1p::nlf-1(+)::GFP, myo-2p::mCherry]*
XZ2010 *nlf-1(ox327) X ; oxEx1149[unc-17p::nlf-1(+) cDNA::GFP, myo-2p::mCherry]*
XZ2011 *nlf-1(ox327) X ; oxEx1155[unc-17Hp::nlf-1(+) cDNA::GFP, myo-2p::mCherry]*
XZ2012 *nlf-1(ox327) X ; oxEx1151[acr-2p::nlf-1(+) cDNA::GFP, myo-2p::mCherry]*
XZ2013 *nlf-1(ox327) X ; oxEx1323[unc-17βp::nlf-1(+) cDNA::GFP, myo-2p::mCherry]*
XZ2014 *nlf-1(ox327) X ; oxEx1152[glr-1p::nlf-1(+) cDNA::GFP, myo-2p::mCherry]*

Table S2. List of plasmids

Miscellaneous plasmids

pCFJ90	*myo-2::mCherry*
pGH47	*unc-17p::mCherry::H2B*
pL15EK	*lin-15(+)*
pWD79-2RV	*hsp-16.48p::FLP*
QT#99	*Phs::GFP-C3T*
F55A4	cosmid carrying the *nlf-1* gene F55A4.2, used to make *oxEx1041* (10 ng/μl)
yk1279a1	*nlf-1* full length cDNA
Litmus 28i	
Litmus 38i	

Gateway entry clones

p_C06E1.4-93	*glr-1p* [4-1] (727 bp of the *glr-1* promoter upstream of and including the ATG)
pADA180	*unc-17Hp* [4-1] (derived from the *unc-17* promoter of pGH1, carrying a 127 bp deletion that removes the nerve cord β enhancer, expressed in head cholinergic neurons)
pCFJ31	*acr-2p* [4-1] (3362 bp of the *acr-2* promoter upstream of the ATG)
pCR110	*GFP* [1-2]
pCR185	*GFP::unc-54* 3'UTR [2-3]
pEntry[2-3]-UTR[unc-54]	*unc-54 3'UTR* [2-3]
pEntry[4-1]-P[rab-3]	*rab-3p* [4-1] (1224 bp of the *rab-3* promoter upstream of and including the ATG)
pGH1	*unc-17p* [4-1] (3229 bp of the *unc-17* promoter upstream of and including the ATG)
pMA1	*nlf-1p* [4-1] (5665 bp of the *nlf-1* promoter upstream of and including the ATG)
pMA2	*nlf-1(+)* gene with introns [1-2]
pMA3	*nlf-1* cDNA [1-2] (derived from yk1279a1)
pMA19	*C3T::unc-54 3'UTR* [2-3]
pMA23	*unc-17βp* [4-1] (a fusion of the *unc-17* nerve cord β enhancer to the minimal *unc-17* promoter consisting of the 382 bp upstream of and including the ATG, expressed in ventral nerve cord cholinergic neurons)
pWD178	*FRT::mCherry::let-858 3'UTR::FRT::GFP* [1-2]

Gateway expression constructs

pMA4	*nlf-1p::GFP*, used to make *oxEx1144* (10 ng/μl)
pMA5	*rab-3p::nlf-1 cDNA::GFP*, used to make *oxEx1146* (10 ng/μl)
pMA6	*nlf-1p::nlf-1(+)::GFP*, used to make *oxEx1147* (10 ng/μl)
pMA8	*unc-17p::nlf-1 cDNA::GFP*, used to make *oxEx1149* (10 ng/μl)
pMA9	*acr-2p::nlf-1 cDNA::GFP*, used to make *oxEx1151* (10 ng/μl)
pMA10	*glr-1p::nlf-1 cDNA::GFP*, used to make *oxEx1152* (10 ng/μl)
pMA11	*unc-17Hp::nlf-1 cDNA::GFP*, used to make *oxEx1155* (10 ng/μl)
pMA27	*rab-3p::FRT::mCherry::let-858 3'UTR::FRT::GFP::C3T::unc-54 3'UTR*, used to make *oxIs412* (10 ng/μl)
pMA28	*unc-17p::FRT::mCherry::let-858 3'UTR::FRT::GFP::C3T::unc-54 3'UTR*, used to make *oxIs414* (10 ng/μl)
pMA39	*unc-17Hp::FRT::mCherry::let-858 3'UTR::FRT::GFP::C3T::unc-54 3'UTR*, used to make *oxIs434* (10 ng/μl)
pMA40	*unc-17βp::FRT::mCherry::let-858 3'UTR::FRT::GFP::C3T::unc-54 3'UTR*, used to mak *oxIs435* (10 ng/μl)
pMA52	*unc-17β::nlf-1 cDNA::GFP*, used to make *oxEx1323* (10 ng/μl)